

Supporting information for:

Origin and control of Chemoselectivity in Cytochrome c-Catalyzed Carbene transfer into Si–H and N–H bonds

Marc Garcia-Borràs,^{1,5,‡,*} S. B. Jennifer Kan,^{3,‡} Russell D. Lewis,^{2,‡} Allison Tang,³ Gonzalo Jimenez-Osés,⁴ Frances H. Arnold,^{2,3,*} K. N. Houk^{1,*}

¹ Department of Chemistry and Biochemistry, University of California, Los Angeles, California 90095, United States.

² Division of Biology and Bioengineering, California Institute of Technology, 1200 East California Blvd, Pasadena, California 91125, United States.

³ Division of Chemistry and Chemical Engineering 210-41, California Institute of Technology, 1200 East California Blvd, Pasadena, California 91125, United States.

⁴ CIC bioGUNE, Bizkaia Technology Park, Building 801A, 48170 Derio, Spain

⁵ Institut de Química Computacional i Catàlisi (IQCC) and Departament de Química, Universitat de Girona, Carrer Maria Aurèlia Capmany 69, 17003 Girona, Spain.

‡Denotes equal author contribution.

†To whom correspondence should be addressed: houk@chem.ucla.edu, frances@cheme.caltech.edu, marcgbq@gmail.com

- I. Materials and Experimental Methods
- II. Computational Methods
 - a. Quantum Mechanics (Density Functional Theory) calculations
 - b. Hybrid Quantum Mechanics/Molecular Mechanics (QM/MM) calculations
 - c. Molecular Dynamics (MD) simulations
- III. General Procedures
 - a. Plasmid construction
 - b. Cytochrome c expression and purification
 - c. Hemochrome assay
 - d. Library construction
 - e. Enzyme library screening
 - f. Protein lysate preparation
 - g. Biocatalytic reactions
 - h. Kinetic time course reactions
 - i. Synthesis and characterization of organosilicon compounds
- IV. Tables and Figures
- V. Supplemental References

I. Materials and Methods

Unless otherwise noted, all chemicals and reagents for chemical reactions were obtained from commercial suppliers (Acros, Arch Bioscience, Fisher Scientific, Sigma-Aldrich, TCI America, VWR) and used without further purification. Multitron shakers (Infors, Annapolis Junction, MD) were used for cell growth. UV-Vis spectroscopy was performed using a Shimadzu UV-1800 spectrophotometer (Shimadzu, Carlsbad, CA). Sonication was performed using a Qsonica Q500 sonicator. Silica gel chromatography purifications were carried out using AMD Silica Gel 60, 230-400 mesh. ^1H NMR spectra were recorded on a Bruker Prodigy 400 MHz instrument and are internally referenced to the residual solvent peak (chloroform). Data for ^1H NMR are reported in the conventional form: chemical shift (δ ppm), multiplicity (s = singlet, d = doublet, t = triplet, q = quartet, hept = heptet, m = multiplet, br = broad, app = appears as), coupling constant (Hz), integration. Gas chromatography (GC) analyses were carried out using an Agilent 7820A gas chromatograph, a flame ionization detector (FID), and J&W HP-5 (30 m x 0.32 mm, 0.25 μm film; 90 $^\circ\text{C}$ hold 1 min, 90 to 110 $^\circ\text{C}$ at 15 $^\circ\text{C}/\text{min}$, 110 to 280 $^\circ\text{C}$ at 60 $^\circ\text{C}/\text{min}$, 280 $^\circ\text{C}$ hold 1 min, 6.2 min total).

Plasmid pET22 was used as a cloning vector, and cloning was performed using Gibson assembly.¹ The cytochrome *c* maturation plasmid pEC86² was used as part of a two-plasmid system to express prokaryotic cytochrome *c* proteins. Cells were grown using Lysogeny Broth medium or HyperBroth (AthenaES, Baltimore, MD) with 100 $\mu\text{g}/\text{mL}$ ampicillin and 20 $\mu\text{g}/\text{mL}$ chloramphenicol ($\text{LB}_{\text{amp/chor}}$ or $\text{HB}_{\text{amp/chor}}$). Primer sequences are available upon request. Electrocompetent *Escherichia coli* cells were prepared following the protocol of Sambrook *et al.*³ T5 exonuclease, Phusion polymerase, and *Taq* ligase were purchased from New England Biolabs (NEB, Ipswich, MA). M9-N minimal medium (abbreviated as M9-N buffer; pH 7.4) was used as a buffering system unless otherwise specified. M9-N minimal medium (abbreviated as M9-N buffer; pH 7.4) was used without a carbon source; it contains 47.7 mM Na_2HPO_4 , 22.0 mM KH_2PO_4 , 8.6 mM NaCl , 2.0 mM MgSO_4 , and 0.1 mM CaCl_2 .

II. Computational Methods

a) Quantum Mechanics (Density Functional Theory) calculations

Density Functional Theory (DFT) calculations were carried out using Gaussian09.⁴ A truncated model containing the porphyrin pyrrole core, Fe center and an imidazole to mimic histidine as Fe-axial ligand was used. Geometry optimizations and frequency calculations were performed using (U)B3LYP⁵⁻⁷ functional with the SDD basis set for iron and 6-31G(d) on all other atoms. Transition states had one negative force constant corresponding to the desired reaction coordinate. All stationary points were verified as minima or first-order saddle points by a vibrational frequency analysis. Intrinsic reaction coordinate (IRC) calculations were performed to ensure that the optimized transition states connect the corresponding desired reactants and products. Enthalpies and entropies were calculated for 1 atm and 298.15 K. A correction to the harmonic oscillator approximation, as discussed by Truhlar and co-workers, was also applied to the entropy calculations by raising all

frequencies below 100 cm^{-1} to 100 cm^{-1} ^{8, 9} using Goodvibes v.1.0.1 python script.¹⁰ Single point energy calculations were performed using the dispersion-corrected functional (U)B3LYP-D3(BJ)^{11, 12} with the Def2TZVP basis set on all atoms, and within the CPCM polarizable conductor model (diethyl ether, $\epsilon = 4$)^{13, 14} to have an estimation of the dielectric permittivity in the enzyme active site. The use of a dielectric constant $\epsilon=4$ has been proved to be a good and general model to account for electronic polarization and small backbone fluctuations in enzyme active sites.^{15, 16}

The methodology employed in this study, based on the use of (U)B3LYP density functional, is very similar to the one used by Shaik group for the study of iron carbene porphyrins,¹⁷ and more recently by Luis, Solà, Costas and co-workers to study non-heme iron carbene transfer reactions,¹⁸ and also by us in our recent studies on carbene transferases.^{19, 20}

(U)B3LYP has also been extensively proved to accurately perform in the computational modeling of iron-oxo chemistry.²¹⁻²⁵

The modeling of the open-shell electronic state was done by using a Gaussian09 “stable = opt” calculation²⁶⁻²⁸ to generate a singlet open-shell orbital guess from the triplet optimized geometry, followed by a full optimization of the system starting from this guess. Although using this approach we could successfully determine the open-shell singlet pathway for the carbene formation step, all the attempts to optimize the carbene Si–H insertion open-shell singlet TS (TS2-OSS) and open-shell singlet amination TSs (N-nucleophilic attack and N–H HAT) were unsuccessful.

Optimized DFT structures are illustrated with CYLView.²⁹

b) Hybrid Quantum Mechanics/Molecular Mechanics (QM/MM) calculations

QM/MM calculations within the ONIOM approach^{30, 31} were carried out using Gaussian09.⁴ Geometry optimizations were performed using (U)B3LYP⁵⁻⁷ functional in combination with the SDD basis set for iron and 6-31G(d) on all other atoms and AmberFF14Sb force field, using the QuadMac algorithm³² as implemented in Gaussian09 and a mechanical embedding scheme. Stationary points were verified as minima by a vibrational frequency analysis. Single point energy calculations were performed at the (U)B3LYP/Def2TZVP:AmberFF14Sb level, and using an electrostatic embedding scheme.

Snapshots for QM/MM calculations were obtained from classical MD trajectories, as described below, and included all the protein residues, cofactors, counterions and water molecules contained in a $<3\text{ \AA}$ shell around the protein structure. QM region (82 atoms) included the heme porphyrin pyrrole core and carboxylate groups, Fe center, a histidine imidazole axial ligand, the carbene atoms, and the bridging water molecule and the corresponding diazo or silane substrates, as done in our previous study.¹⁹ The total charge of the QM region was -2 . In the QM/MM optimizations, the active site region to be optimized included all QM atoms and all the residues and water molecules of the MM region within 6 \AA from any atom in the QM region. The TAO (Toolkit to Assist ONIOM Calculations) package of scripts by Tao and Schlegel³³ was used to assist the preparation and conversion of the necessary files from Amber and pdb formats to Gaussian09 format.

KIE calculations

Kinetic isotope effects (KIE) were calculated using the Onyx program (Brueckner, A. C.; Ogba, O. M.; Cevallos, S. L.; Walden, D. M.; O’Leary, D. J. ; Cheong, P. H.-Y. Onyx, version 1.0; Oregon State University: Corvallis, OR, USA, 2016). KIE values are obtained from the Bigeleisen-Mayer method, where the lowest in energy open-shell singlet (OSS) IPC and OSS TDE-IPC structures were considered as ground states for the truncated and QM/MM systems, respectively, and at the same level of theory used for the optimizations described early.

c) Molecular Dynamics (MD) simulations

Molecular Dynamics simulations were performed using the GPU code (*pmemd*)³⁴ of the AMBER 16 package.³⁵ Parameters for the IPC were generated within the *antechamber* and *MCPB.py*³⁶ modules in AMBER16 package using the general AMBER force field (*gaff*),³⁷ with partial charges set to fit the electrostatic potential generated at the B3LYP/6-31G(d) level by the RESP model.³⁸ The charges were calculated according to the Merz–Singh–Kollman scheme^{39, 40} using the Gaussian 09 package.⁴ Protonation states of protein residues were predicted using H++ server. Each protein was immersed in a pre-equilibrated truncated cuboid box with a 10 Å buffer of TIP3P⁴¹ water molecules using the *leap* module, resulting in the addition of around 6,400 solvent molecules. The systems were neutralized by addition of explicit counter ions (Na⁺ and Cl⁻). All subsequent calculations were done using the widely tested Stony Brook modification of the Amber14 force field (*ff14sb*).⁴² A two-stage geometry optimization approach was performed. The first stage minimizes the positions of solvent molecules and ions imposing positional restraints on the solute by a harmonic potential with a force constant of 500 kcal·mol⁻¹·Å⁻² and the second stage minimizes all the atoms in the simulation cell except those involved in the harmonic distance restraint. The systems were gently heated using six 50 ps steps, incrementing the temperature by 50 K for each step (0–300 K) under constant-volume and periodic-boundary conditions. Water molecules were treated with the SHAKE algorithm such that the angle between the hydrogen atoms was kept fixed. Long-range electrostatic effects were modelled using the particle-mesh-Ewald method.⁴³ An 8 Å cutoff was applied to Lennard–Jones and electrostatic interactions. Harmonic restraints of 30 kcal·mol⁻¹ were applied to the solute and the Andersen equilibration scheme was used to control and equalize the temperature. The time step was kept at 1 fs during the heating stages, allowing potential inhomogeneities to self-adjust. Each system was then equilibrated for 2 ns with a 2 fs time step at a constant volume. Production trajectories were then run for an additional 500 or 1000 ns (0.5 or 1 μs) under the same simulation conditions. Trajectories were processed and analyzed using the *cpptraj*⁴⁴ module from Ambertools utilities. Snapshots for QM/MM calculations were obtained from a clusterization analysis of MD trajectories using *cpptraj*, where a representative snapshot from the most populated cluster was selected.

Constrained-MD simulations included a restrained distance between the amine N atom in silane substrate **6** and the IPC central C atom (2.5 Å), that was defined by adding an harmonic potential with $k = 100 \text{ mol}^{-1} \text{ Å}^{-2}$ to this coordinate during the respective equilibrations and production runs.

Umbrella Sampling Molecular Dynamics (US-MD) simulations

Umbrella sampling MD (US-MD) simulations were carried out using AMBER16 package and the equivalent protocol, force field, and parameters as described earlier for the regular MD simulations, but using a 1 fs time step during equilibration and production run. To generate the potential mean force (PMF), a reaction coordinate defined by the distance between the center of mass of the silane substrate **1** and the central C atom of the IPC was used. A total of 500 ns production run was accumulated for each US-MD simulation, consisting of 90 windows distributed along the silane binding coordinate from a distance of 12.8 Å (unbound silane) to 4.0 Å (silane-bound complex), and using a 0.1 Å increment between each window. Simulations within each window were restrained using an harmonic potential with $k = 200 \text{ mol}^{-1} \text{ Å}^{-2}$. A minimization of the system, followed by an equilibration run of 1 ns (not included in the PMF calculation) preceded each window production run. The minimized and equilibrated configuration from the previous window (window i) was used to start the simulation of the next window (window $i + 1$). US-MD simulations were initiated from the most populated cluster of each enzyme variant with the IPC bound obtained from previous MD simulations, where silane **1** was placed in a random position in the solvent box, 12.8 Å away from the IPC central C atom. The Weighted Histogram Analysis Method⁴⁵⁻⁴⁷ (WHAM) was used to reweigh the biased histograms obtained from the US-MD simulations.

III. General Procedures

a) Plasmid construction

All variants described in this paper were cloned and expressed using the pET22(b)+ vector (MilliporeSigma, St. Louis, MO). The gene encoding *Rhodothermus marinus* *cyt c* V75T M100D M103E (*Rma* TDE) was obtained as a single gBlock (Integrated DNA Technologies, Coralville, IA),⁴⁸ codon-optimized for *E. coli*, and cloned using Gibson assembly¹ into pET22(b)+ between restriction sites *NdeI* and *XhoI* in frame. The gene encoding *Rma* TDE contained an *N*-terminal pelB leader sequence and 6xHisTag (MKYLLPTAAAGLLLLAAQPAMAHHHHHH) and had the first seven amino acids of mature, wild-type *Rma* *cyt c* removed (TESGTAA). This plasmid was co-transformed with the cytochrome *c* maturation plasmid pEC86² into *E. coli*[®] EXPRESS BL21(DE3) cells (Lucigen, Middleton, WI).

DNA coding sequence of *Rma* *cyt c* V75T M100D M103E with an *N*-terminal pelB leader sequence and 6xHisTag:

```
ATGAAATACCTGCTGCCGACCGCTGCTGCTGGTCTGCTGCTCCTCGCTGCCAG
CCGGCGATGGCCATCATCATCACCACCAAGACCCGGAAGCACTGGCAGC
GGAAATTGGTCCGGTCAAACAGGTGAGCCTGGGTGAACAGATTGATGCGGCC
TGGCGCAACAGGGAGAACAGCTCTTCAACACGTATTGTAAGTGCCTGCCACCGT
CTGGATGAGCGTTTTATCGGACCGGCCCTGCGCGATGTTACCAAACGTCGTGGG
CCGGTTTACATCATGAACACGATGCTGAACCCGAATGGGATGATCCAGCGTCA
```

TCCGGTGATGAAACAGCTCGTGCAGGAATATGGGACCATGGATAACCGATGAGG
CCCTGAGTGAAGAACAAGCGCGCAATTCTGGAGTATCTGCGCCAGGTTGCG
GAAAACCAGTAATGA

Amino acid sequence of *Rma cyt c* V75T M100D M103E with an *N*-terminal pelB leader sequence and 6xHisTag:

MKYLLPTAAAGLLLLLAAQPAMAHHHHHHQQDPEALAAEIGPVKQVSLGEQIDAAL
AQQGEQLFNTYCTACHRLDERFIGPALRDVTKRRGPVYIMNTMLNPNNGMIQRHPV
MKQLVQEYGTMDTDEALSEEQARAILEYLRQVAENQ

DNA coding sequence of *Rma cyt c* V75T N80F M99P M100D M103I with an *N*-terminal pelB leader sequence and 6xHisTag:

ATGAAATACCTGCTGCCGACCGCTGCTGCTGGTCTGCTGCTCCTCGCTGCCAG
CCGGCGATGGCCCATCATCATCACCACCAAGACCCGGAAGCACTGGCAGC
GGAAATTGGTCCGGTCAAACAGGTGAGCCTGGGTGAACAGATTGATGCGGCC
TGGCGCAACAGGGAGAACAGCTCTTCAACACGTATTGTACTGCGTGCCACCGT
CTGGATGAGCGTTTTATCGGACCGGCCCTGCGCGATGTTACCAAACGTCGTGGG
CCGGTTTACATCATGAACACGATGCTGAACCCGTTTGGGATGATCCAGCGTCAT
CCGGTGATGAAACAGCTCGTGCAGGAATATGGGACCATGGATCCGGATATTGC
CCTGAGTGAAGAACAAGCGCGCAATTCTGGAGTATCTGCGCCAGGTTGCGG
AAAACCAGTAATGA

Amino acid sequence of *Rma cyt c* V75T N80F M99P M100D M103I with an *N*-terminal pelB leader sequence and 6xHisTag:

MKYLLPTAAAGLLLLLAAQPAMAHHHHHHQQDPEALAAEIGPVKQVSLGEQIDAAL
AQQGEQLFNTYCTACHRLDERFIGPALRDVTKRRGPVYIMNTMLNPFNGMIQRHPV
MKQLVQEYGTMDPDIALSEEQARAILEYLRQVAENQ

b) Cytochrome *c* expression and purification

Purified cytochrome *c* proteins were prepared as follows. In a 4 L flask, one liter HyperBroth (AthenaES) containing 100 µg/mL ampicillin and 20 µg/mL chloramphenicol (HB_{amp/chlor}) was inoculated with an overnight culture (20 mL, Lysogeny Broth, with 100 µg/mL ampicillin, 20 µg/mL chloramphenicol, LB_{amp/chlor}) of recombinant *E. cloni*[®] EXPRESS BL21(DE3) cells containing a pET22(b)+ plasmid encoding the cytochrome *c* variant, and the pEC86 plasmid. The culture was shaken at 37 °C and 200 rpm (no humidity control) until the OD₆₀₀ was 0.7 (approximately 3 hours). The culture was placed on ice for 30 minutes, and isopropyl β-D-1-thiogalactopyranoside (IPTG) and 5-aminolevulinic acid (ALA) were added to final concentrations of 20 µM and 200 µM, respectively.

The incubator temperature was reduced to 25 °C, and the culture was allowed to shake for 20 hours at 200 rpm. Cells were harvested by centrifugation (4 °C, 15 min, 4,000xg), and the cell pellet was stored at -20 °C until further use (at least 24 hours). The cell pellet was

resuspended in buffer containing 100 mM NaCl, 20 mM imidazole, and 20 mM sodium phosphate buffer (pH 7.5) and cells were lysed by sonication (4 minutes, 1 second on, 1 second off, 30% duty cycle; Qsonica Q500 sonicator). Cell lysate was placed in a 75 °C heat bath for 10 minutes, and afterwards cell debris was removed by centrifugation for 20 min (30,000xg, 4 °C). Supernatant was sterile-filtered through a 0.45 µm cellulose acetate filter and purified using a 1 mL Ni-NTA column (HisTrap HP, GE Healthcare, Piscataway, NJ) using an AKTA purifier FPLC system (GE Healthcare). The cytochrome *c* protein was eluted from the column by running a gradient from 20 to 500 mM imidazole over 10 column volumes.

The purity of the collected cytochrome *c* fractions was analyzed using sodium dodecyl sulfate-polyacrylamide gel electrophoresis (SDS-PAGE). Pure fractions were pooled and concentrated using a 3 kDa molecular weight cut-off centrifugal filter. Protein was dialyzed overnight into 20 mM sodium phosphate buffer (pH 7.5) using 3.5 kDa molecular weight cut-off dialysis tubing. The dialyzed protein was further concentrated using a 3 kDa molecular weight cut-off centrifugal filter, flash-frozen on dry ice, and stored at -80 °C. The concentration of cytochrome *c* was determined in triplicate using the hemochrome assay described in section (c).

c) Hemochrome assay

A solution of sodium dithionite (100 mM) was prepared in M9-N buffer. Separately, a solution of 1 M NaOH (0.4 mL) was mixed with pyridine (1 mL), followed by centrifugation (10,000xg, 30 seconds) to separate the excess aqueous layer gave a pyridine-NaOH solution. To a cuvette containing 10 µL purified protein solution and 640 µL M9-N buffer, 100 µL of dithionite solution and 250 µL pyridine-NaOH solution were added. The cuvette was sealed with Parafilm, and the UV-Vis spectrum was recorded immediately at room temperature between 600 and 380 nm on a UV-1800 Shimadzu spectrophotometer. Cytochrome *c* concentration was determined using $\epsilon_{550-535} = 22.1 \text{ mM}^{-1}\text{cm}^{-1}$.^{48, 49}

d) Library construction

Cytochrome *c* site-saturation mutagenesis libraries were generated using a modified version of the 22-codon site-saturation method.⁵⁰ For each site-saturation library, oligonucleotides were ordered such that the coding strand contained the degenerate codon NDT, VHG or TGG. The reverse complements of these primers were also ordered. The three forward primers were mixed together in a 12:9:1 ratio, (NDT:VHG:TGG) and the three reverse primers were mixed similarly. Two PCRs were performed, pairing the mixture of forward primers with a pET22(b)+ internal reverse primer, and the mixture of reverse primers with a pET22b internal forward primer. The two PCR products were gel purified, ligated together using Gibson assembly,¹ and transformed into *E. coli*[®] EXPRESS BL21(DE3) cells. Primer sequences are available upon request.

e) Enzyme library screening

Single colonies were picked with toothpicks off of LB_{amp/chlor} agar plates, and grown in deep-well (2 mL) 96-well plates containing LB_{amp/chlor} (400 μ L) at 37 °C, 250 rpm shaking, and 80% relative humidity overnight. After 16 hours, 30 μ L aliquots of these overnight cultures were transferred to deep-well 96-well plates containing HB_{amp/chlor} (1 mL) using a 12-channel EDP3-Plus 5-50 μ L pipette (Rainin). Glycerol stocks of the libraries were prepared by mixing cells in LB_{amp/chlor} (100 μ L) with 50% v/v glycerol (100 μ L). Glycerol stocks were stored at -78 °C in 96-well microplates. Growth plates were allowed to shake for 3 hours at 37 °C, 250 rpm shaking, and 80% relative humidity. The plates were then placed on ice for 30 min. Cultures were induced by adding 10 μ L of a solution, prepared in sterile deionized water, containing 2 mM IPTG and 20 mM ALA. The incubator temperature was reduced to 24 °C, and the induced cultures were allowed to shake for 20 hours (250 rpm, no humidity control). Cells were pelleted (4,000xg, 5 min, 4 °C) and resuspended in 450 μ L M9-N buffer. For cell lysis, plates were placed in a 75 °C water bath for 10 min, followed by centrifugation (4,000xg, 5 min, 4 °C) to remove cell debris. The resulting heat-treated lysates (320 μ L) were then transferred to deep-well plates for biocatalytic reactions. In an anaerobic chamber, to deep-well plates of heat-treated lysates were added 40 μ L Na₂S₂O₄ (100 mM in dH₂O), and 40 μ L reactant solution (100 mM phenyl(dimethyl)silane, 100 mM 4-isopropylaniline, 150 mM Me-EDA in MeCN). The plates were sealed with aluminum sealing tape, removed from the anaerobic chamber, and shaken at 400 rpm for 1.5 h. Reactions were quenched with acetonitrile (400 μ L), and allowed to sit at room temperature for 30 minutes to allow proteins to precipitate from solution. The plates were centrifuged (5,000xg, 10 min) and the organic layer (400 μ L) was transferred to shallow-well 96-well plates for reverse phase HPLC analysis. Protein variants that displayed improved selectivity for the 4-isopropylaniline substrate were then regrown in shake flasks, and evaluated for their activity and selectivity with 4-dimethylsilylaniline in small-scale biocatalytic reactions, which were analyzed by GC for accurate determination of turnovers and chemoselectivity.

f) Protein lysate preparation

Protein lysates for biocatalytic reactions were prepared as follow: *E. coli* cells expressing *Rma* cyt *c* variant were pelleted (4,000xg, 5 min, 4 °C), resuspended in M9-N buffer and adjusted to the appropriate optical density at 600 nm (OD₆₀₀). The whole-cell solution was sonicated, (1 minute, 1 second on, 1 second off, 30% duty cycle) heat-treated (75 °C for 10 min) and then centrifuged (14,000xg, 10 min, 4 °C) to remove cell debris. The supernatant was sterile filtered through a 0.45 μ m cellulose acetate filter, concentration of cytochrome *c* protein in the lysate was determined using the hemochrome assay described in section (C). Using this protocol, the protein concentrations we typically observed for OD₆₀₀ = 30 lysates were in the 3-15 μ M range.

g) Biocatalytic reactions

In an anaerobic chamber, heat-treated cell lysate containing an *Rma* cyt *c* variant was diluted to concentration of 1.2 μ M with M9-N buffer, and 340 μ L of this solution was transferred to a 2 mL crimp vial. Next, the protein was reduced by adding 40 μ L Na₂S₂O₄ (100 mM in M9-

N buffer), and the reaction was initiated with the addition of reactants, 10 μL the appropriate silane solution (400 mM in MeCN) and 10 μL Me-EDA (400 mM in MeCN). The vial was crimp sealed, removed from the anaerobic chamber, and shaken at 400 rpm at room temperature for 2 hours. At the end of the reaction, the crimp vial was opened and the reaction was quenched with cyclohexane (1 mL). Internal standard was added (20 μL of 20 mM 1,2,3-trimethoxybenzene in toluene or 20 μL of 20 mM 2-phenylethanol in toluene) and the reaction mixture was transferred to a microcentrifuge tube, vortexed (1 minute), then centrifuged (14,000xg, 5 min) to completely separate the organic and aqueous layers. The organic layer (800 μL) was removed for GC and chiral HPLC analysis. All biocatalytic reactions were performed in triplicate. The total turnover numbers (TTNs) reported are calculated with respect to the protein catalyst and represent the total number of turnovers obtained using the catalyst under the stated reaction conditions.

Concentration of organosilicon product was calculated based on the ratio of areas between the product peak and internal standard peak, as measured by GC-FID.

Stock solutions of chemically synthesized authentic standard organosilicon products were prepared at various concentrations (20 to 200 mM in MeCN). To a microcentrifuge tube were added 340 μL M9-N buffer, 40 μL $\text{Na}_2\text{S}_2\text{O}_4$ (100 mM in M9-N buffer), 20 μL organosilicon product, 20 μL internal standard (20 mM 1,2,3-trimethoxybenzene in toluene or 20 μL of 20 mM 2-phenylethanol in toluene) and 1 mL cyclohexane. The mixture was vortexed (1 minute) then centrifuged (14,000xg, 5 min) to completely separate the organic and aqueous layers. The organic layer (800 μL) was removed for GC analysis. Each concentration was prepared in duplicate, and both data points are shown for each concentration (Figure S3). The standard curves plot product concentration in mM (x-axis) against the ratio of product area to internal standard area on the GC (y-axis).

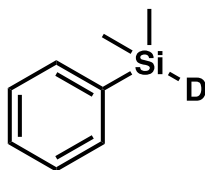
h) Kinetic time course reactions

In an anaerobic chamber, purified protein was added to 3400 μL of M9-N buffer in a 6 mL headspace vial with a magnetic stir bar. Next, the protein was reduced by adding 400 μL $\text{Na}_2\text{S}_2\text{O}_4$ (100 mM in M9-N) and the reaction was initiated with the addition of reactants, 100 μL PhMe_2SiH (400 mM in MeCN) and 100 μL Me-EDA (400 mM in MeCN). At two minute intervals (2, 4, 6, 8, and 10 min) 400 μL of the reaction solution was removed the 6 mL vial, and was transferred to a microcentrifuge tube containing 1000 μL cyclohexane and an internal standard (20 μL of 20 mM 1,2,3 trimethoxybenzene in toluene). The microcentrifuge tube was vortexed for 30 seconds, and then allowed to sit until all samples from all time points had been produced. At the end of the kinetic time course reaction, the microcentrifuge tubes were centrifuged (14,000xg, 1 min) to completely separate the organic and aqueous layers. The organic layer (800 μL) was removed for GC analysis. All biocatalytic reactions were performed in triplicate or quadruplicate. The initial rates reported are calculated with respect to the protein catalyst and represent the number of turnovers per minute per enzyme, obtained using the enzyme under the stated reaction conditions.

i) Synthesis and characterization of organosilicon compounds

Phenyl(dimethyl)-silane-*d* (S1)

Phenyl(dimethyl)-silane-*d* was prepared by adapting a procedure for the hydrogenation of chlorosilanes by NaBH₄.⁵¹ In a 100 mL-round bottom flask, 2.5 g sodium borodeuteride (NaBD₄, 60 mmol, 2.0 equiv., Cambridge Isotope Labs) were added. The flask was purged with argon, and 30 mL anhydrous acetonitrile was added. Under anaerobic conditions, 5.0 g phenyl(dimethyl)silyl chloride (30 mmol, 1 equiv.) was added dropwise over 30 minutes at room temperature, with continuous stirring. The round bottom flask became very hot over the addition of phenyl(dimethyl)silyl chloride, and so slower addition than performed here, and/or addition at 0 °C is recommended for a safer procedure. After completing the addition of the phenyl(dimethyl)silyl chloride, the reaction was allowed to stir at room temperature for an additional 30 min. The reaction was then cooled to 0 °C, after which the flask was opened to aerobic atmosphere and quenched with dropwise addition of saturated aqueous ammonium chloride (NH₄Cl, approximately 10 mL). Purification by silica column chromatography using 100% pentane as an eluent afforded phenyl(dimethyl)-silane-*d* with 61% yield.



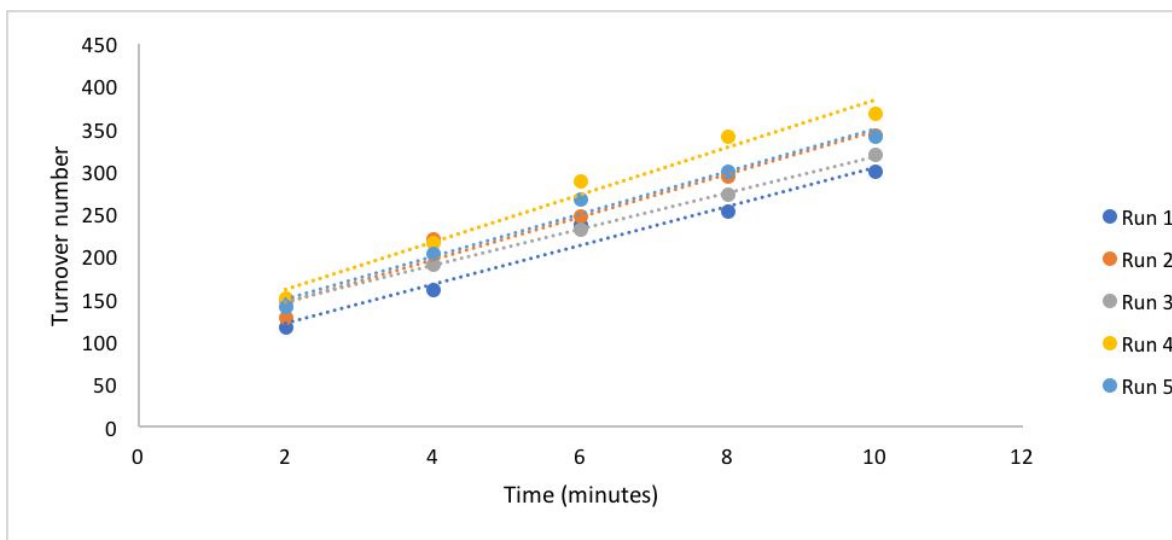
Compound S1. Phenyl(dimethyl)silane-*d*

¹H NMR (400 MHz, CDCl₃) δ 7.48-7.62 (m, 2H), 7.30-7.44 (m, 3H), 0.35 (app q, *J* = 0.6 Hz, 6H).

All other compounds were synthesized as described in ref. ⁴⁸.

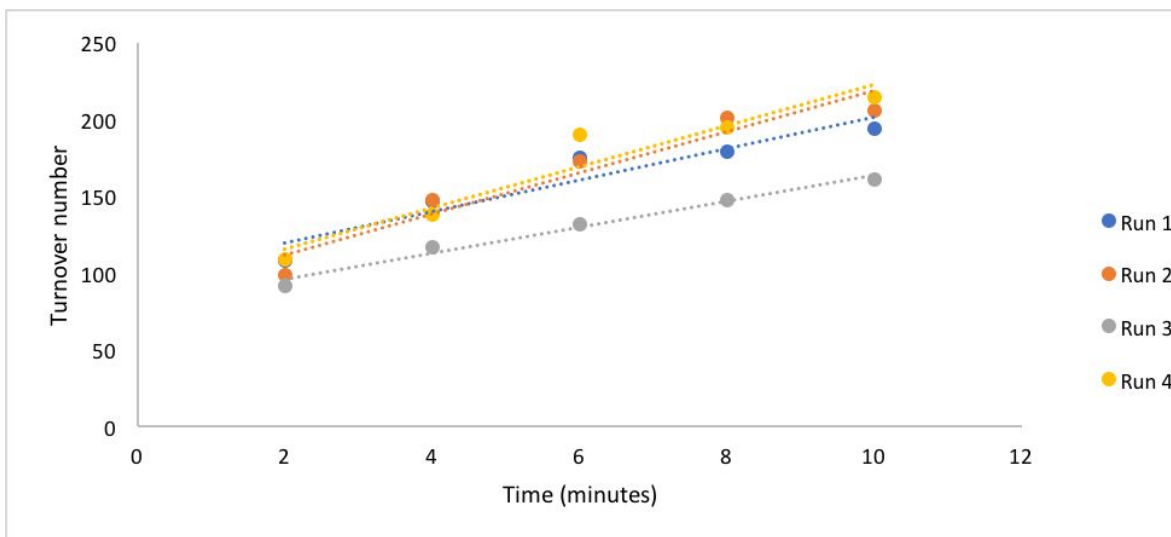
IV. Figures and Tables:

Figure S1. Kinetic time course data for reaction between ethyl 2-diazopropanoate and phenyl(dimethyl)-silane ($\text{PhMe}_2\text{Si-H}$ or $\text{PhMe}_2\text{Si-D}$, as specified), catalyzed by *Rma* cytochrome *c* variants.



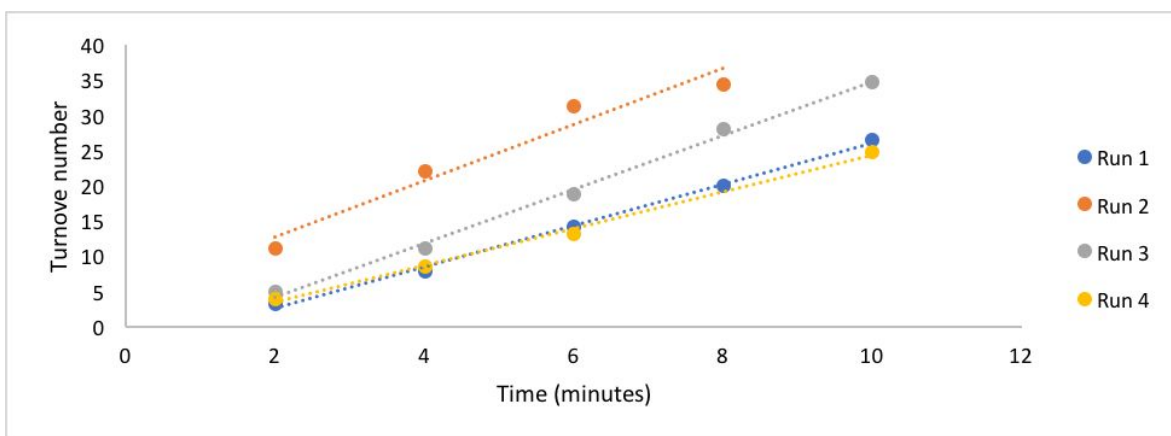
A. Kinetic time course data for reaction using *Rma* TDE and $\text{PhMe}_2\text{Si-H}$. Five independent runs are shown, and the corresponding turnover frequencies are summarized in the table below.

<i>Rma</i> TDE ($\text{PhMe}_2\text{Si-H}$)	
Run 1	25.0 /min
Run 2	21.2 /min
Run 3	27.9 /min
Run 4	25.0 /min
Run 5	22.9 /min
Average	24.4 /min



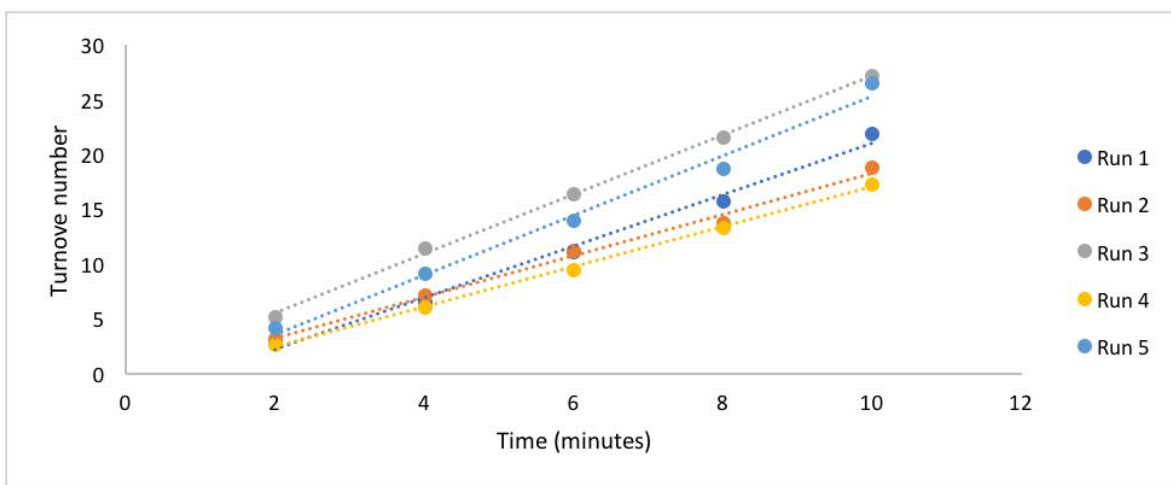
B. Kinetic time course data for reaction using *Rma* TDE and PhMe₂Si-D. Four independent runs are shown, and the corresponding turnover frequencies are summarized in the table below.

<i>Rma</i> TDE (PhMe ₂ Si-D)	
Run 1	10.2 /min
Run 2	13.4 /min
Run 3	8.4 /min
Run 4	13.0 /min
Average	11.3 /min



C. Kinetic time course data for reaction using wild-type *Rma* cyt *c* and PhMe₂Si-H. Four independent runs are shown, and the corresponding turnover frequencies are summarized in the table below.

Wild-type <i>Rma</i> cyt <i>c</i> (PhMe ₂ Si-H)	
Run 1	4.0 /min
Run 2	3.8 /min
Run 3	2.6 /min
Run 4	2.9 /min
Average	3.3 /min



D. Kinetic time course data for reaction using wild-type *Rma* cyt *c* and PhMe₂Si-H. Five independent runs are shown, and the corresponding turnover frequencies are summarized in the table below.

Wild-type <i>Rma</i> cyt <i>c</i> (PhMe ₂ Si-D)	
Run 1	2.3 /min
Run 2	1.9 /min
Run 3	2.7 /min
Run 4	1.8 /min
Run 5	2.7 /min
Average	2.3 /min

Figure S2. ^1H NMR for phenyl(dimethyl)silane and phenyl(dimethyl)silane-*d*.
 ^1H NMR (400 MHz, CDCl_3)

Top spectrum: δ 7.48-7.62 (m, 2H), 7.30-7.44 (m, 3H), 0.35 (app q, $J = 0.6$ Hz, 6H).

Bottom spectrum: δ 7.48-7.62 (m, 2H), 7.30-7.44 (m, 3H), 4.36-4.50 (m, 1H), 0.28-0.42 (m, 6H).

The absence of peak C (4.36-4.50 ppm) in the top spectrum indicates that the Si-H bond has been replaced by a Si-D bond.

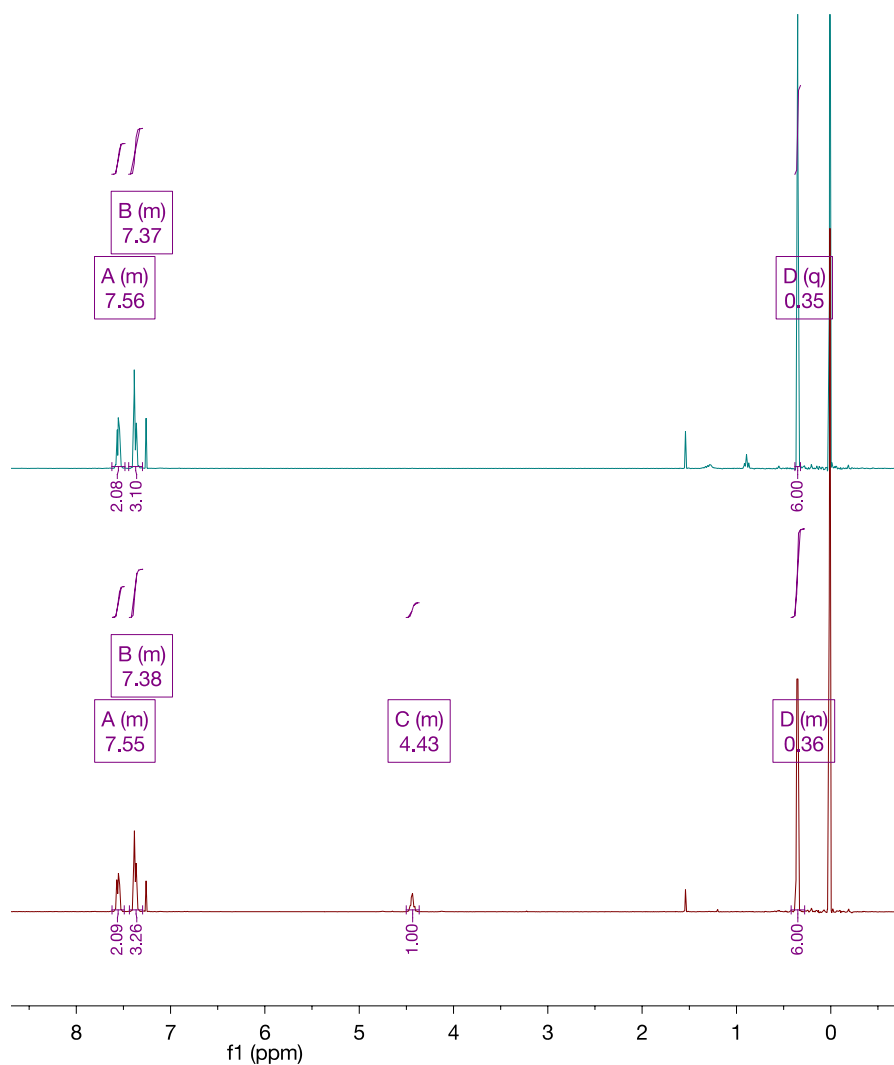


Figure S3. GC Standard curve for ethyl 2-(dimethylphenylsilyl)propanoate product.

The analysis of product formation in enzymatic reactions was performed based on GC standard curves. The standard curve use to quantify the kinetic time course reactions is shown below; all other standard curves were prepared and used as described in reference 48.

Stock solutions of chemically synthesized organosilicon products at various concentrations (20 to 200 mM in MeCN) were prepared. To a microcentrifuge tube were added 340 μ L M9-N buffer, 40 μ L NaS₂O₄ (100 mM in dH₂O), 20 μ L organosilicon product, 20 μ L internal standard (20 mM of 1,2,3 trimethoxybenzene in toluene) and 1 mL cyclohexane. The mixture was vortexed (10 seconds, 3 times) then centrifuged (14,000xg, 5 min) to completely separate the organic and aqueous layers. The organic layer (750 μ L) was removed for GC analysis. All data points represent the average of duplicate runs. The standard curves plot product concentration in mM (x-axis) against the ratio of product area to internal standard area on the GC (y-axis).

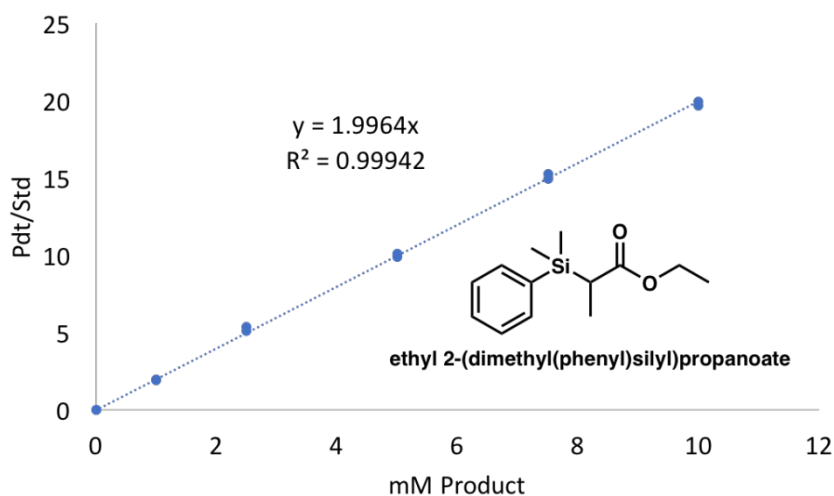
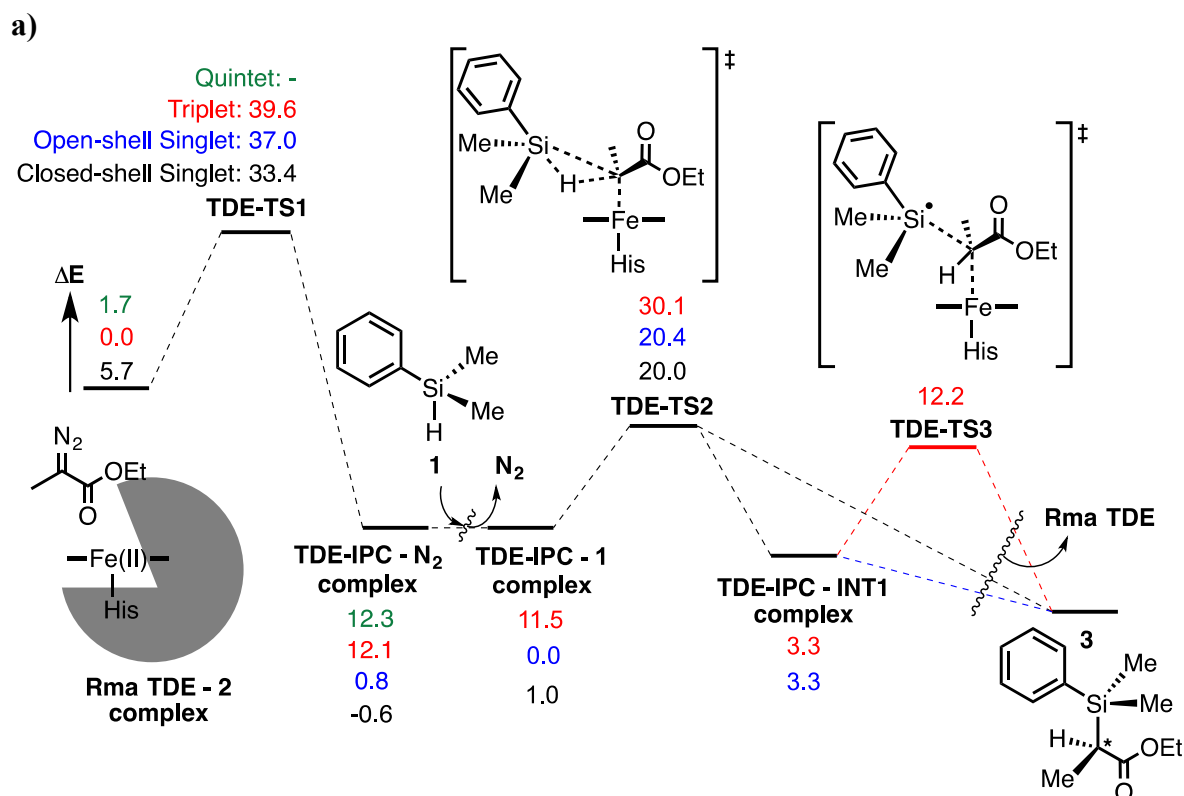


Figure S4. a) Computed reaction pathway for carbene Si–H insertion reaction between PhMe₂SiH **1** and Me-EDA **2** catalyzed by *Rma* TDE at QM/MM level. Three different electronic states are considered: closed-shell singlet (CSS), open-shell singlet (OSS), and triplet (T). For initial *Rma* TDE - **2** complex and TDE-IPC – N₂ complex, the quintet (Q) electronic state was explored. **b)** QM/MM optimized structures for TDE-TS2. Only atoms in the QM region are shown for clarity. Electronic energies are given in kcal·mol⁻¹. Key distances and angles are shown in Å and degrees, respectively.



Closed-shell singlet (CSS) Si–H insertion is found to follow a concerted pathway through **TDE-TS2**, while open-shell singlet (OSS) and triplet(T) electronic states follow a stepwise Si–H insertion mechanism, where a diradical intermediate **TDE-IPC – INT1** is formed. A final step to form the new C–Si bond takes place through **TDE-TS3** along the triplet pathway; whereas a barrierless C–Si bond formation is found to occur along the OSS pathway.

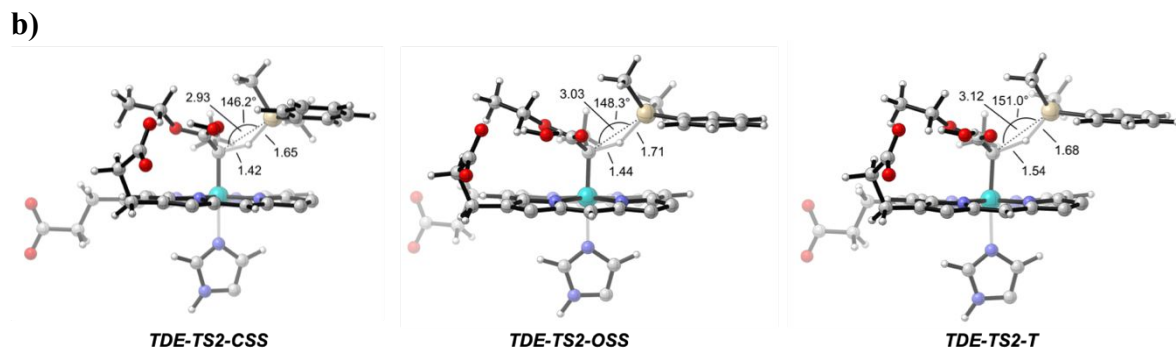


Figure S5. Computed reaction pathway for carbene Si–H insertion reaction between PhMe₂SiH **1** and Me-EDA **2** catalyzed by a model imidazole-ligated iron porphyrin (truncated QM-model) considering the triplet (T) electronic state. As opposite to the closed-shell singlet (CSS) lowest energy pathway, the triplet (T) carbene Si–H insertion occurs via a two-step mechanism: first, hydrogen abstraction from the silane to the carbene takes place (**TS2-T**), forming a diradical intermediate **INT1**; finally the new Si–C bond is formed through the lower energy transition state **TS3-T**. Electronic and quasi-harmonic corrected Gibbs free energies are given in kcal·mol⁻¹. Key distances and angles are shown in Å and degrees, respectively.

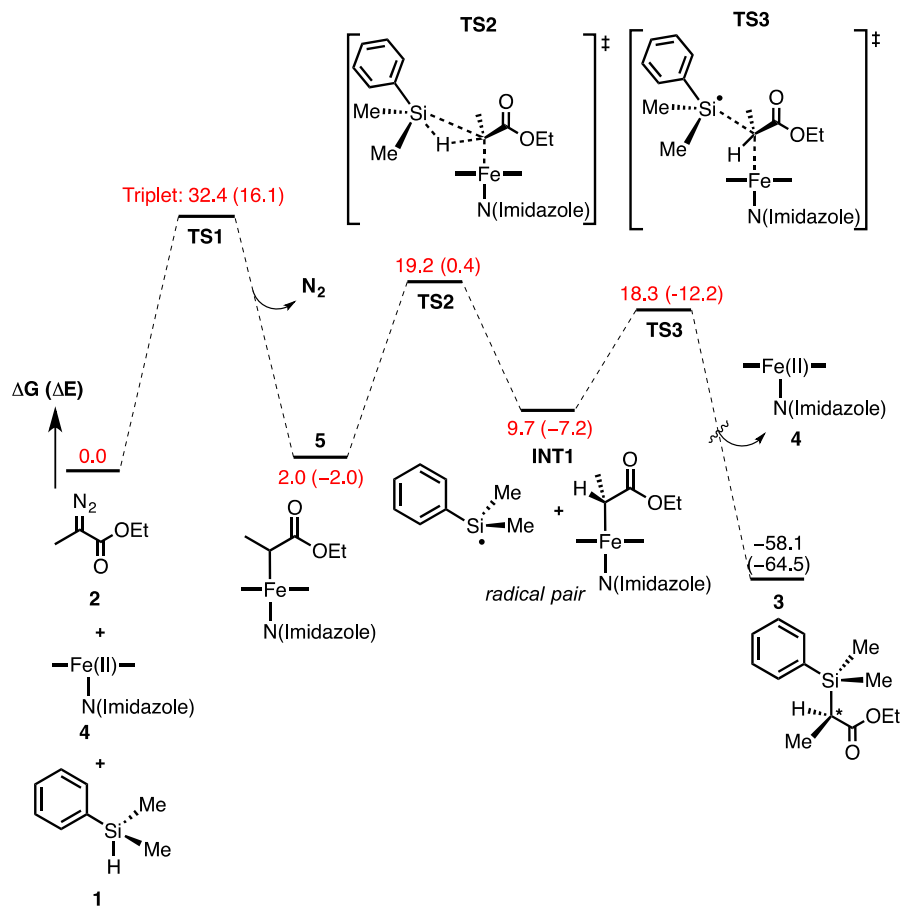
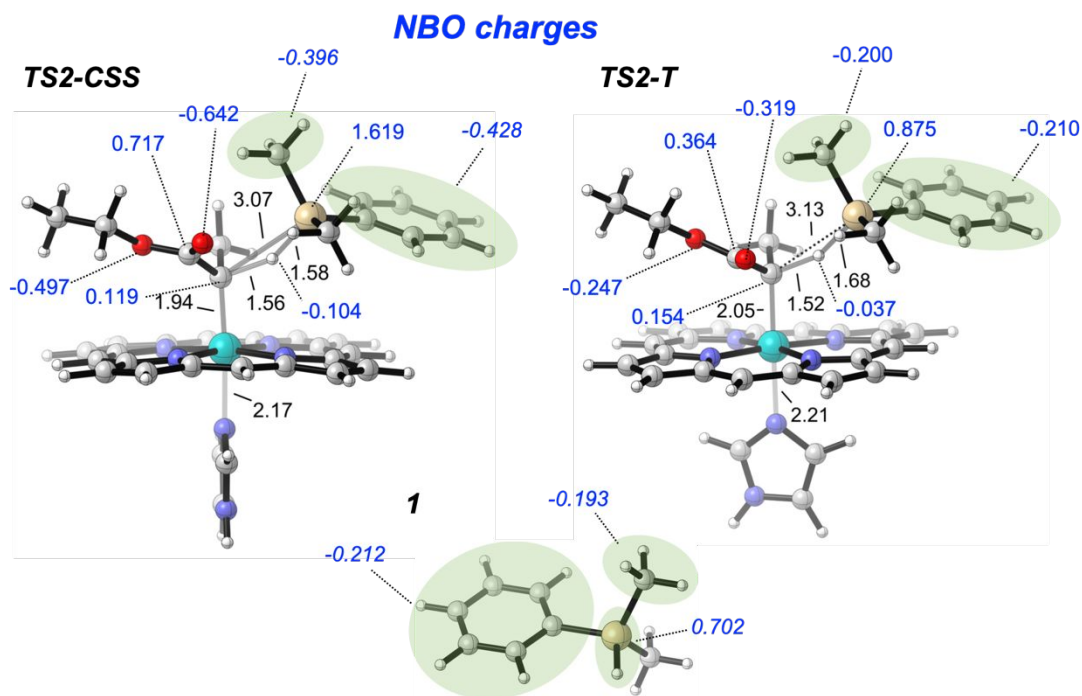


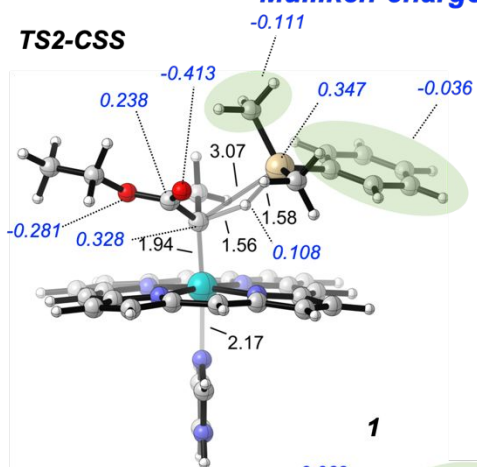
Figure S6. Mulliken and NBO charge distribution and Mulliken spin density analysis for the optimized carbene Si–H carbene insertion transition states for the closed-shell singlet (**TS2-CSS**) and triplet (**TS2-T**) electronic states (truncated QM-model). Charges (in blue), and spin densities (in parenthesis, in blue) are given in a.u.. Charge distribution in silane **1** is shown for comparison. A positive charge on the Si atom is generated in **TS2-CSS**, while a radical Si center is formed in **TS2-T**.

A partial positive charge is accumulated on the silicon atom in **TS2-CSS**, consistent with previous Hammett analysis of the *Rma* TDE-catalyzed reaction: when the relative reaction rates of various *para*-substituted aryldimethylsilanes were plotted against the Hammett σ values for the corresponding *para*-substituents, the calculated ρ value for *Rma* TDE was -0.70 (indicating a partial positive charge build-up on the Si atom in the rate-determining transition state).² This ρ value is larger than those reported for Rh and Cu-based catalysts, for which ρ is -0.31 and -0.54 , respectively.^{12, 13}

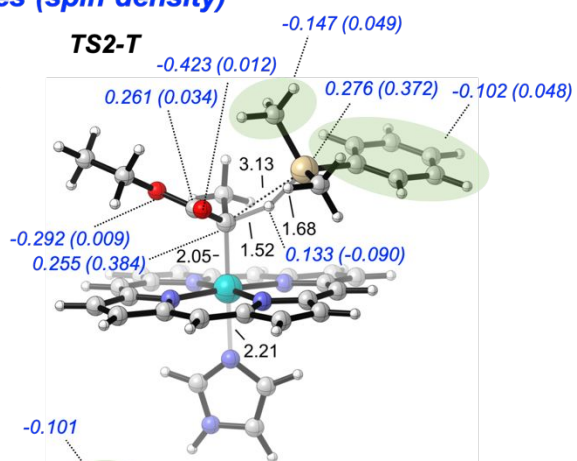


Mulliken charges (spin density)

TS2-CSS



TS2-T



1

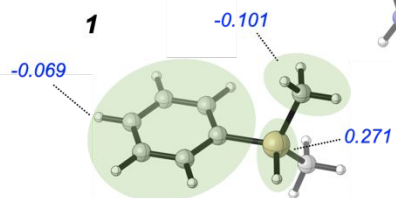


Figure S7. Umbrella Sampling Molecular Dynamics (US-MD) simulations. **a)** Potential of mean force (PMF) measured along the reaction coordinate defined as the distance between the IPC central C atom and the center of mass of the silane substrate **1** for wild-type *Rma* cyt *c* and *Rma* TDE IPC variants. **c)** Representative snapshots of the PMF reaction coordinate obtained from the *Rma* TDE PMF simulations.

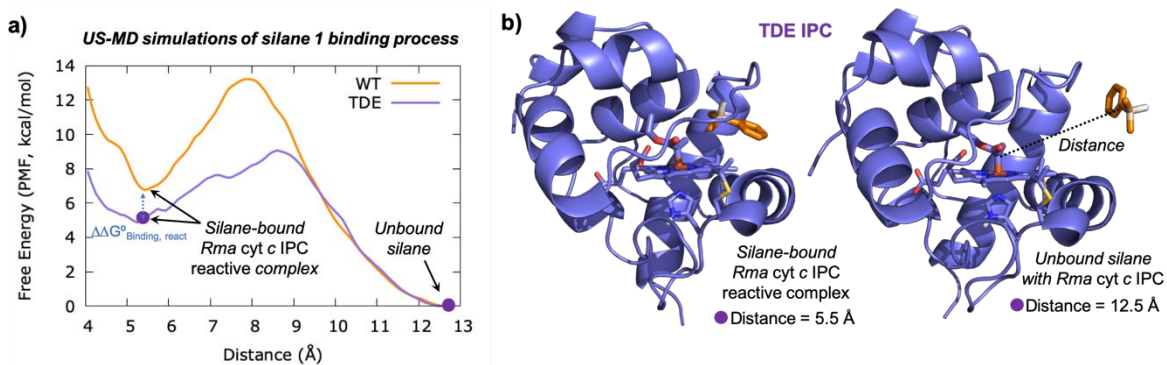
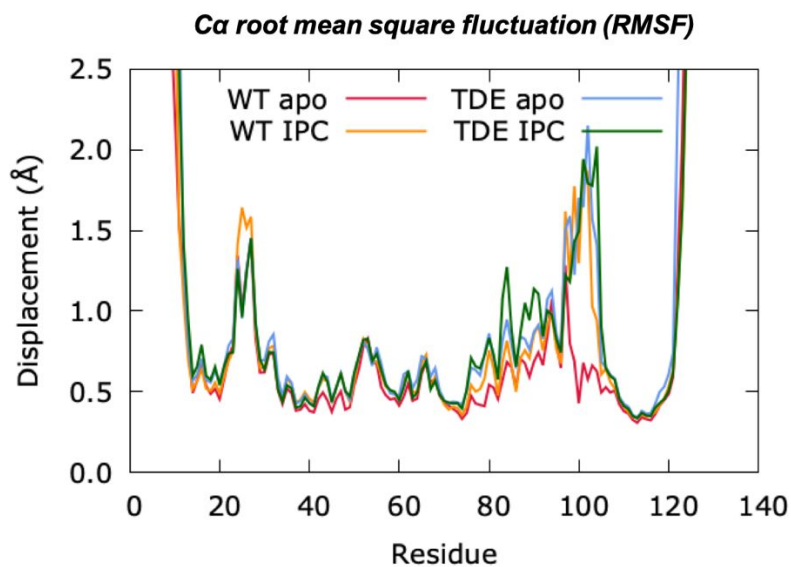
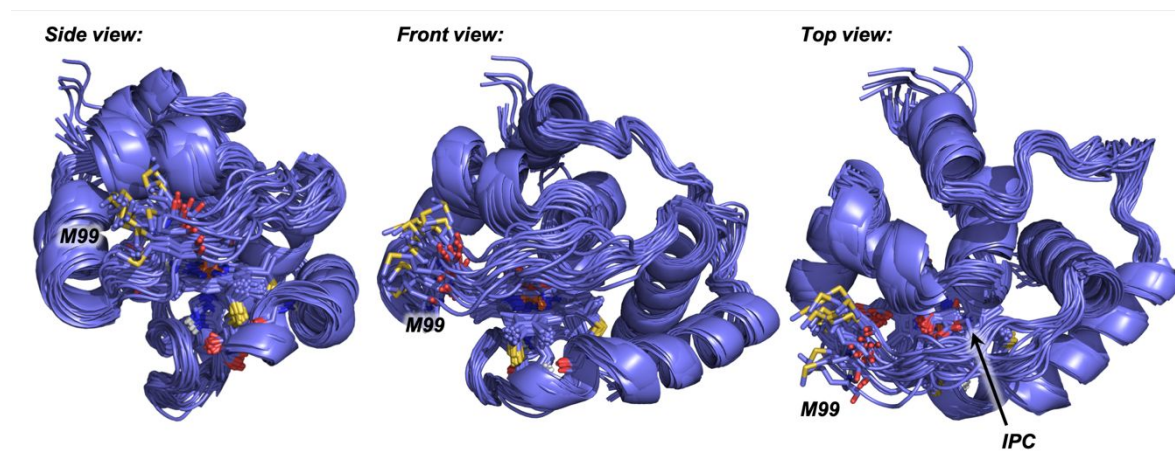


Figure S8. Root mean square fluctuation (RMSF) of protein C α positions measured along 500 ns MD simulations for wild-type *Rma* cyt *c* apo (red) and bound IPC (orange), and *Rma* TDE apo (cyan) and bound IPC (green), that are shown in **Figure 2d** in the main text.



*New mutations in TDE and the formation of the IPC
increase the front loop flexibility*

Figure S9. Overlay of representative snapshots (every 20 ns) obtained from a 1000 ns MD trajectory of *Rma* TDE IPC bound. M99 residue in the front loop is shown in sticks representation.



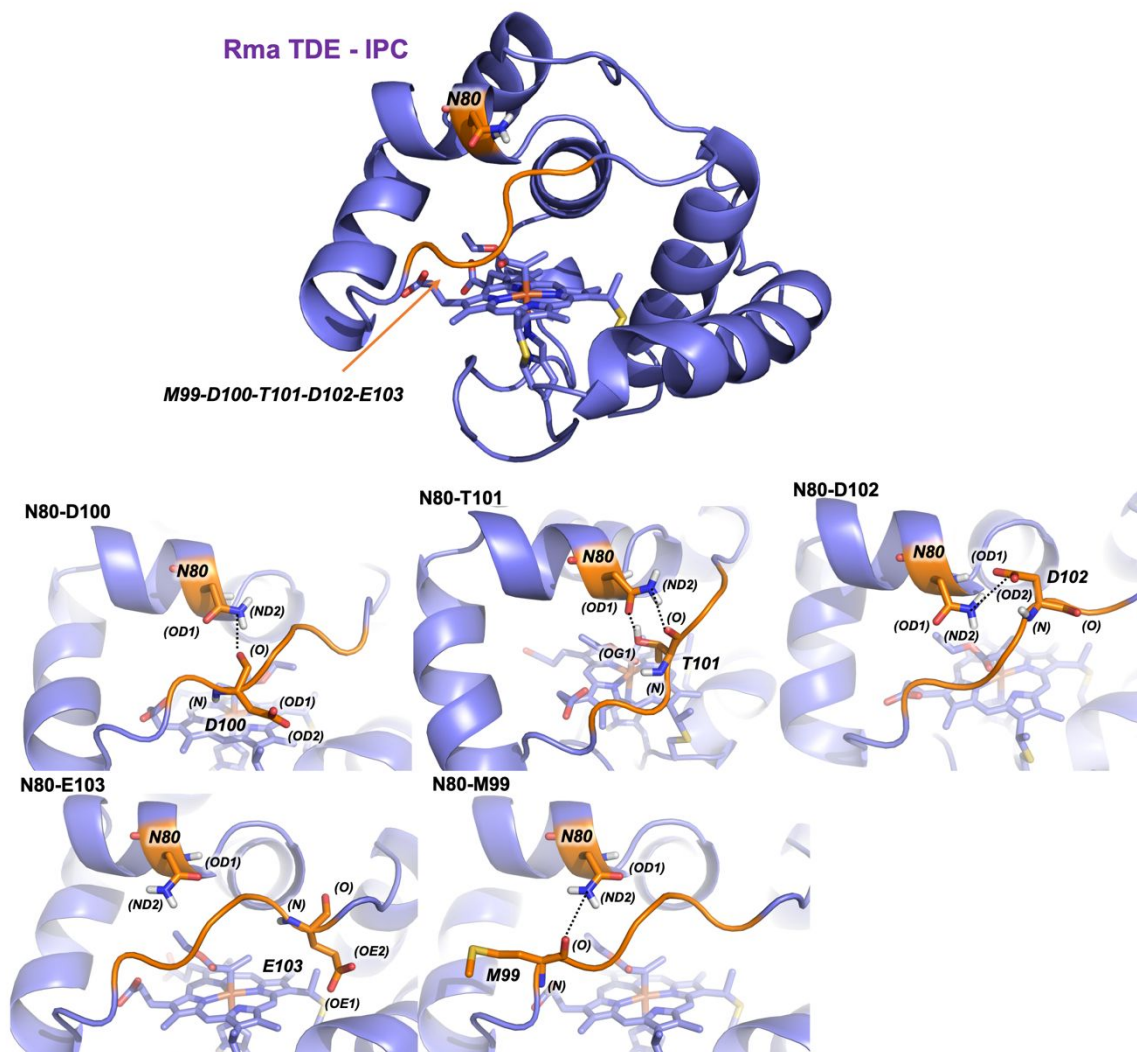
M99 side chain is displaced from the active site of the protein when the iron-carbene is formed and it is forced to be exposed to the solvent. This change on M99 side chain conformation modifies the front loop backbone and directly impacts on the entire loop conformational dynamics.

Figure S10. a) Analysis of key interactions between N80 residue and front loop residues (M99-D100-T101-D102-E103) in TDE-IPC. H-bond interactions between N80 side chain and residues 99-103 (backbone heteroatoms and side chains) were analyzed in 5 independent MD trajectories (**b, c, d, e, and f**, 1000 ns each). Distances around 3 Å between heteroatoms (N, O) are considered as effective H-bond interactions.

Although the E103 residue was found to be far from N80 and no interactions were observed, significant interactions between N80 and other residues were observed to be able to take place along the different MD simulation replicas:

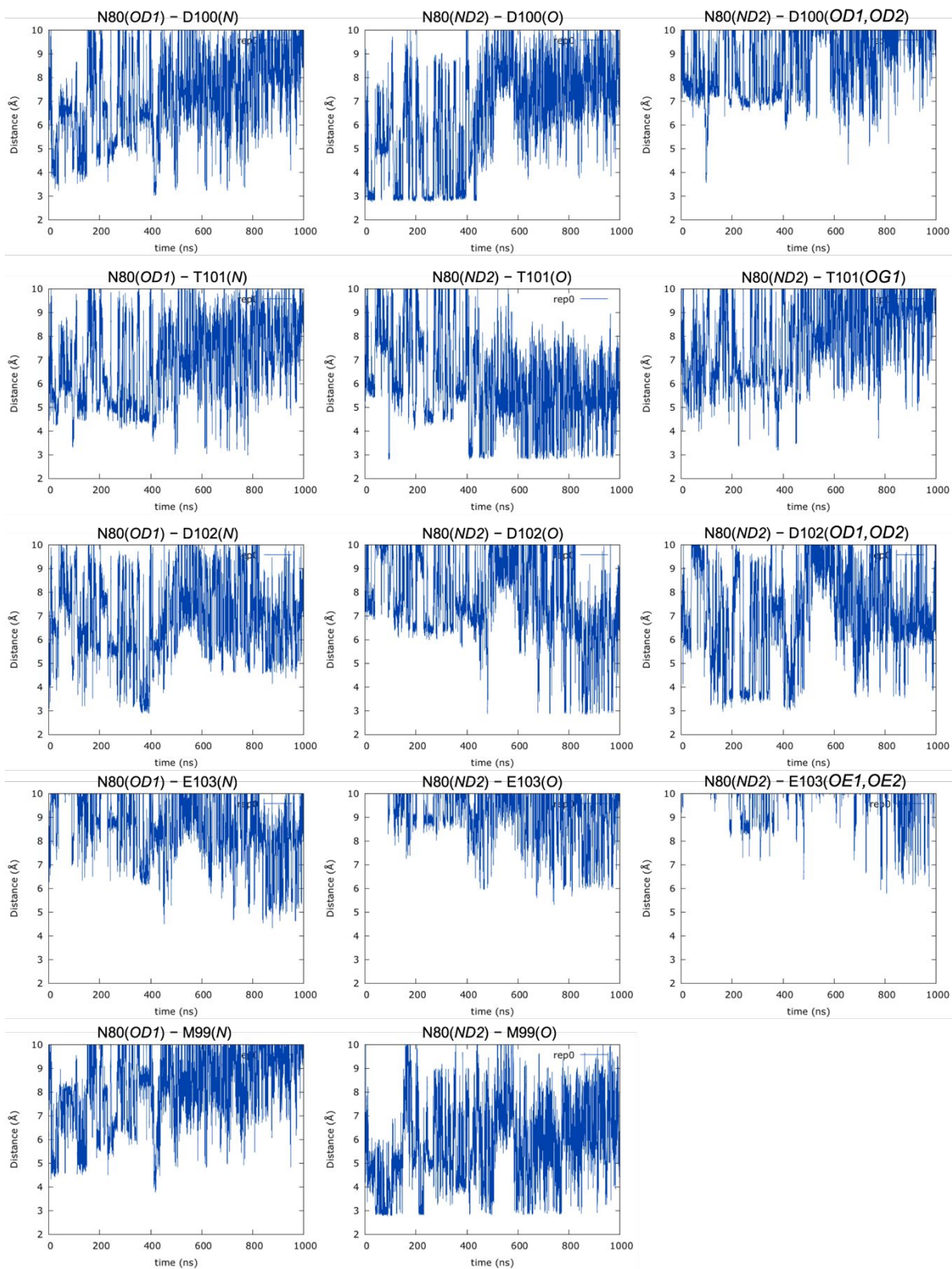
- H-bond between N80(ND2) and backbone carbonyl O from M99, D100, T101, and D102.
- H-bond between N80(OD1) and backbone amide N from D100, T101, and D102.
- H-bond between N80 and side chains from D100(OD1,OD2), T101(OG1), and D102(OD1,OD2).

a)



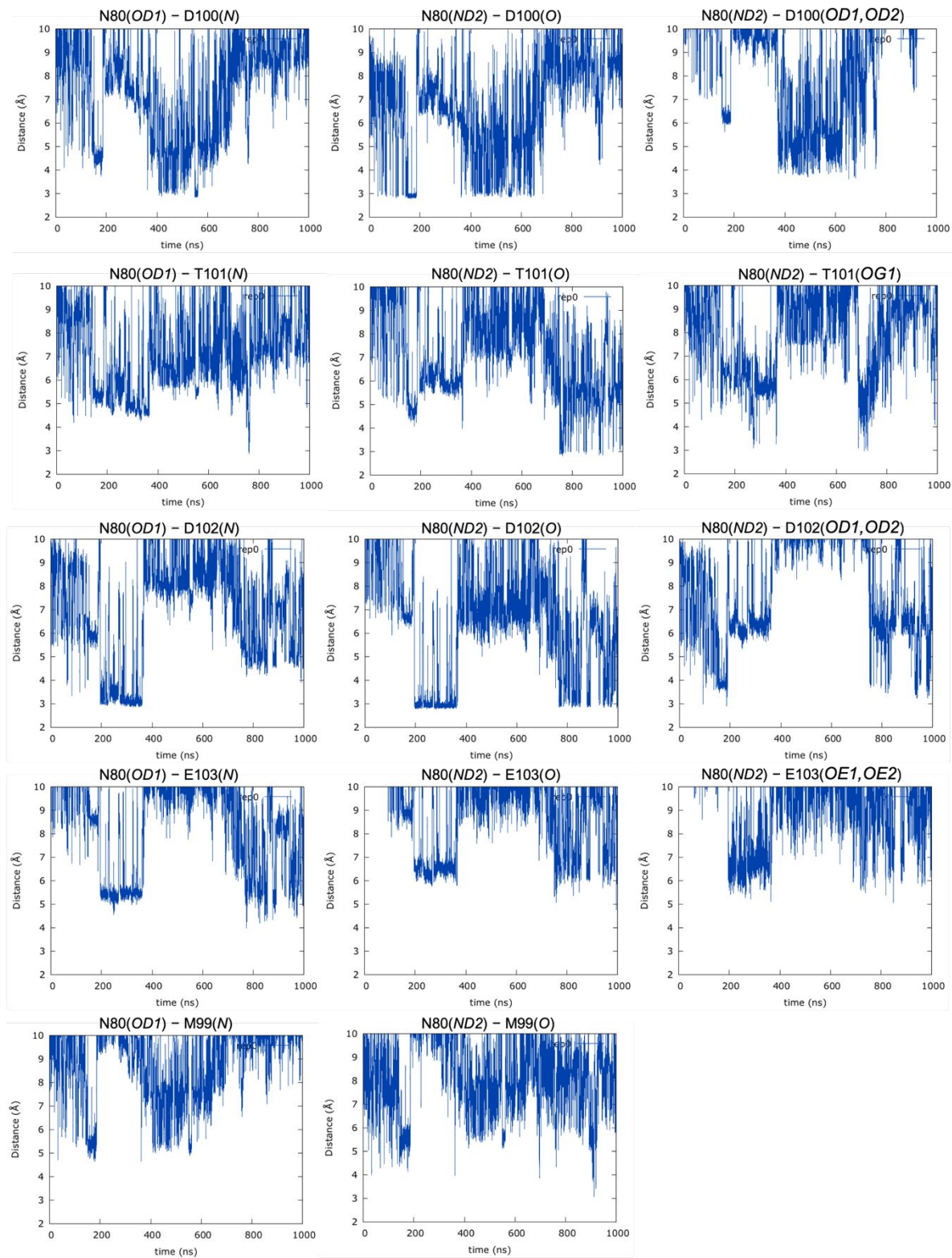
b)

Replica 0:



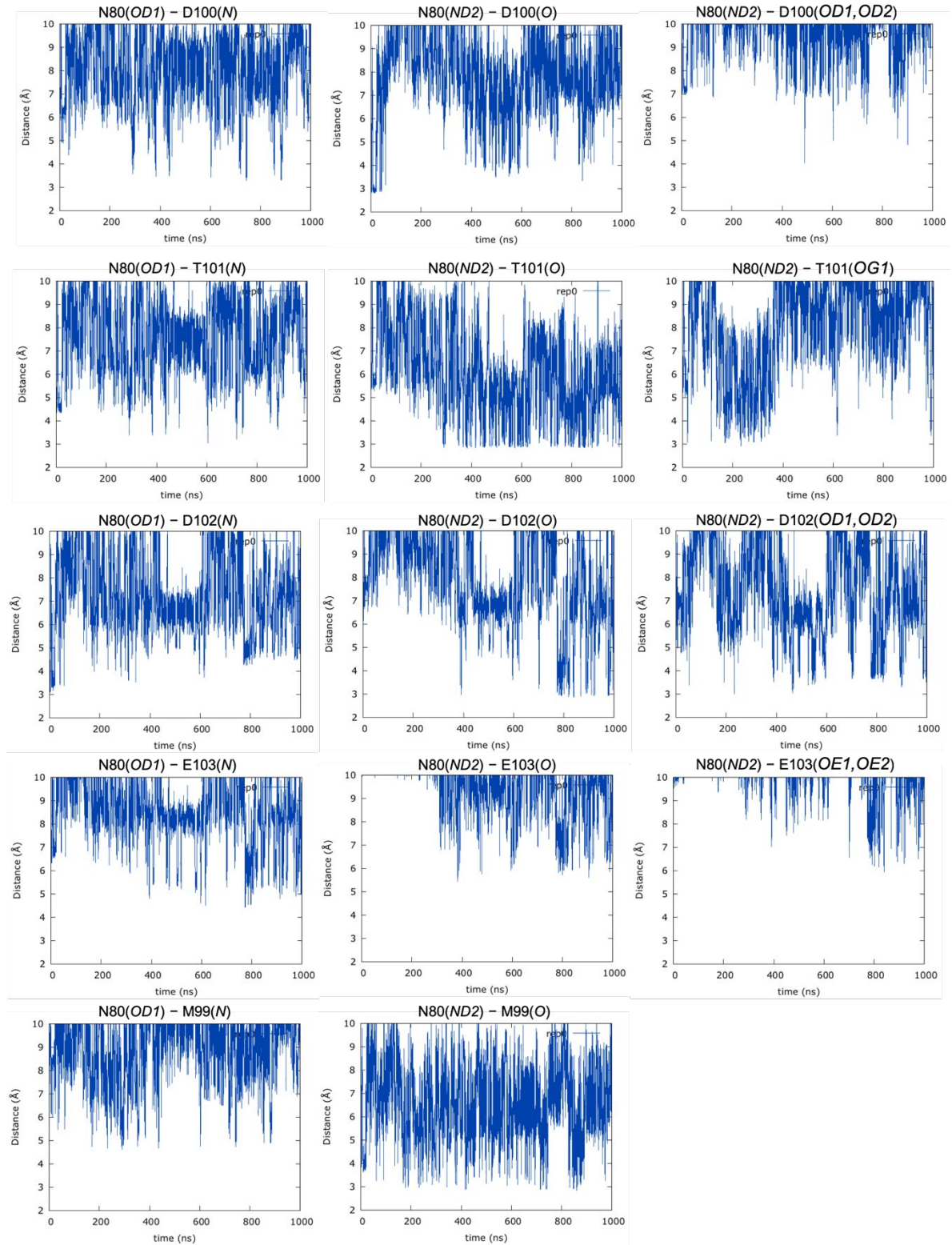
c)

Replica 1:



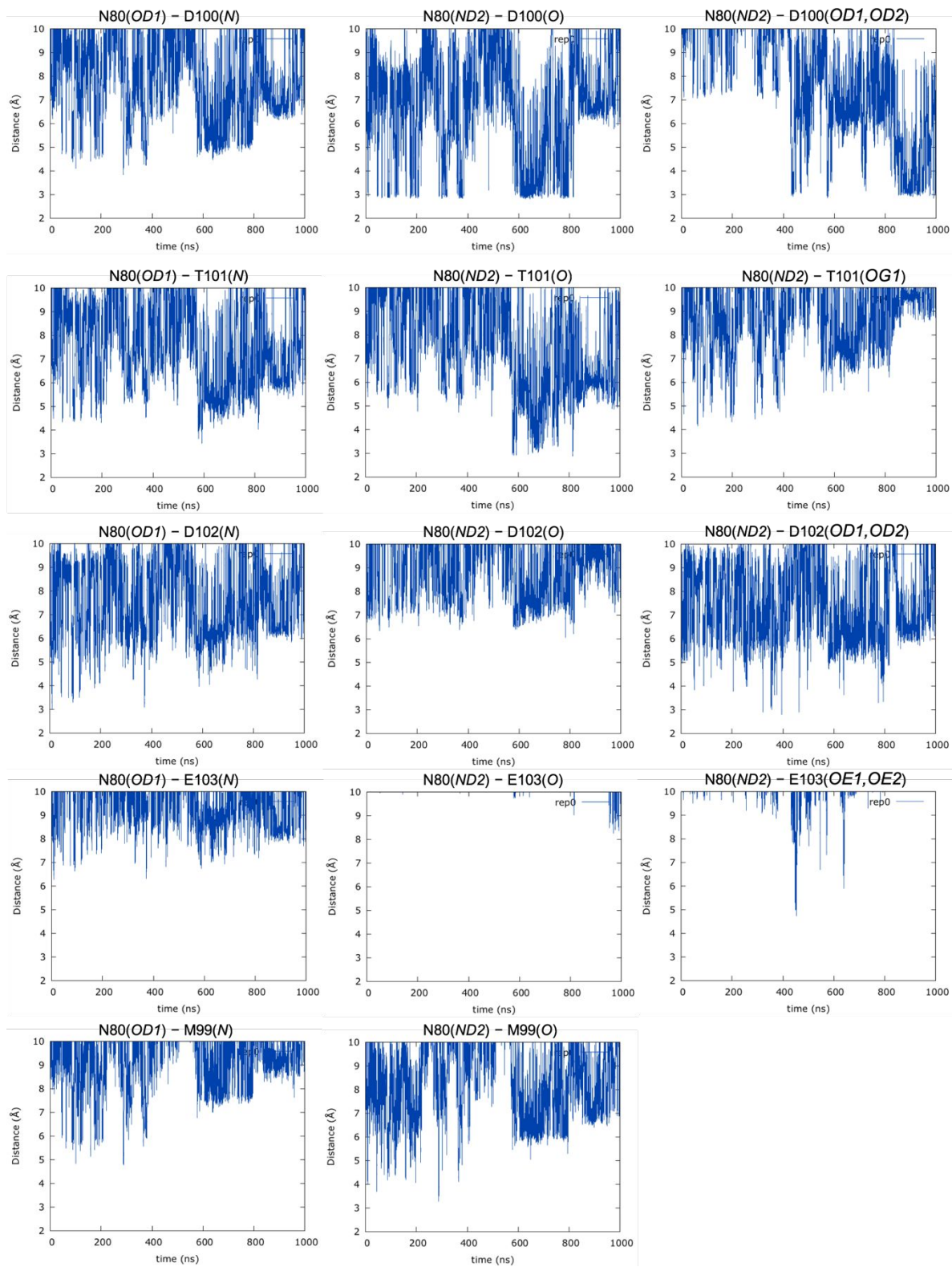
d)

Replica 2:



e)

Replica 3:



f)

Replica 4:

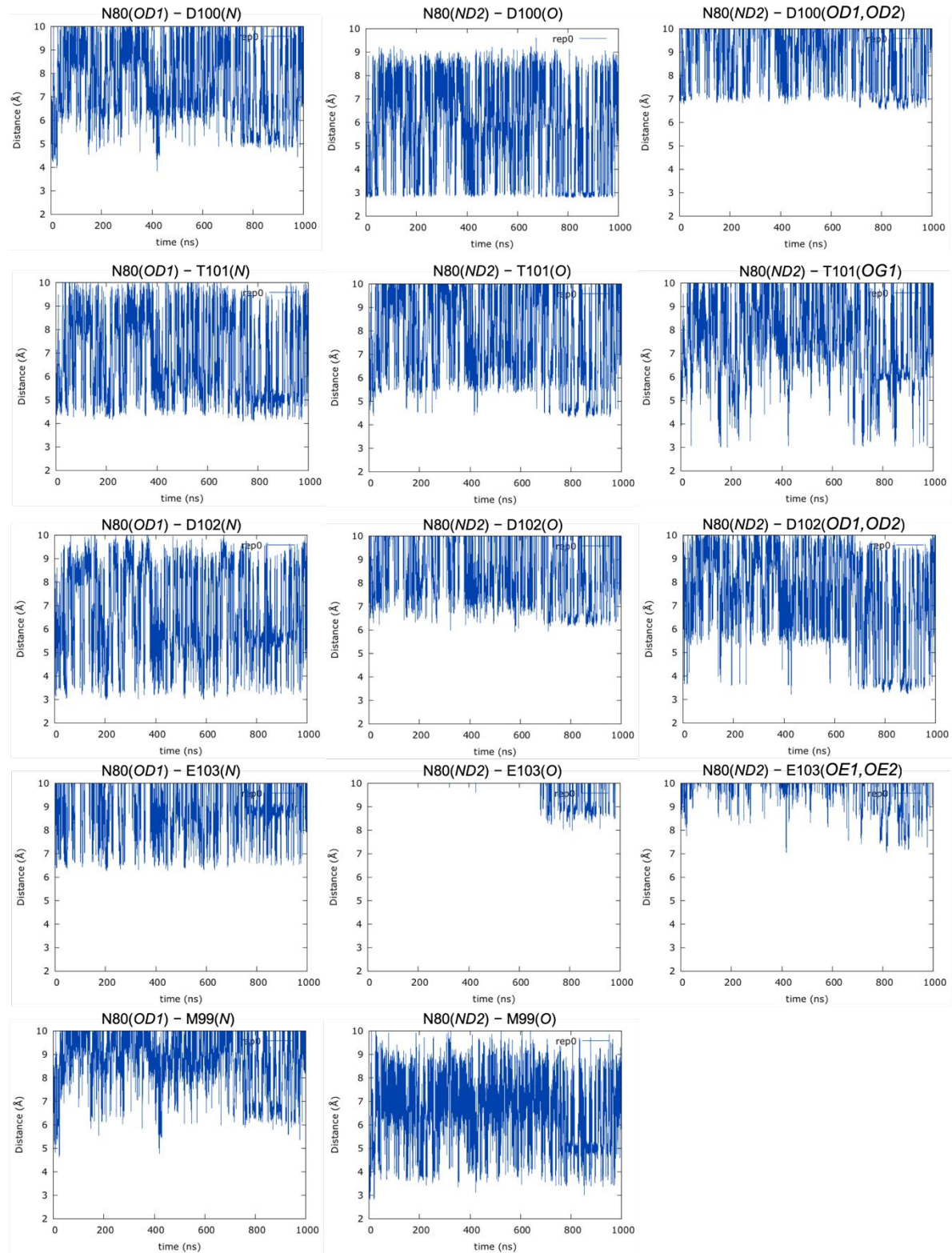
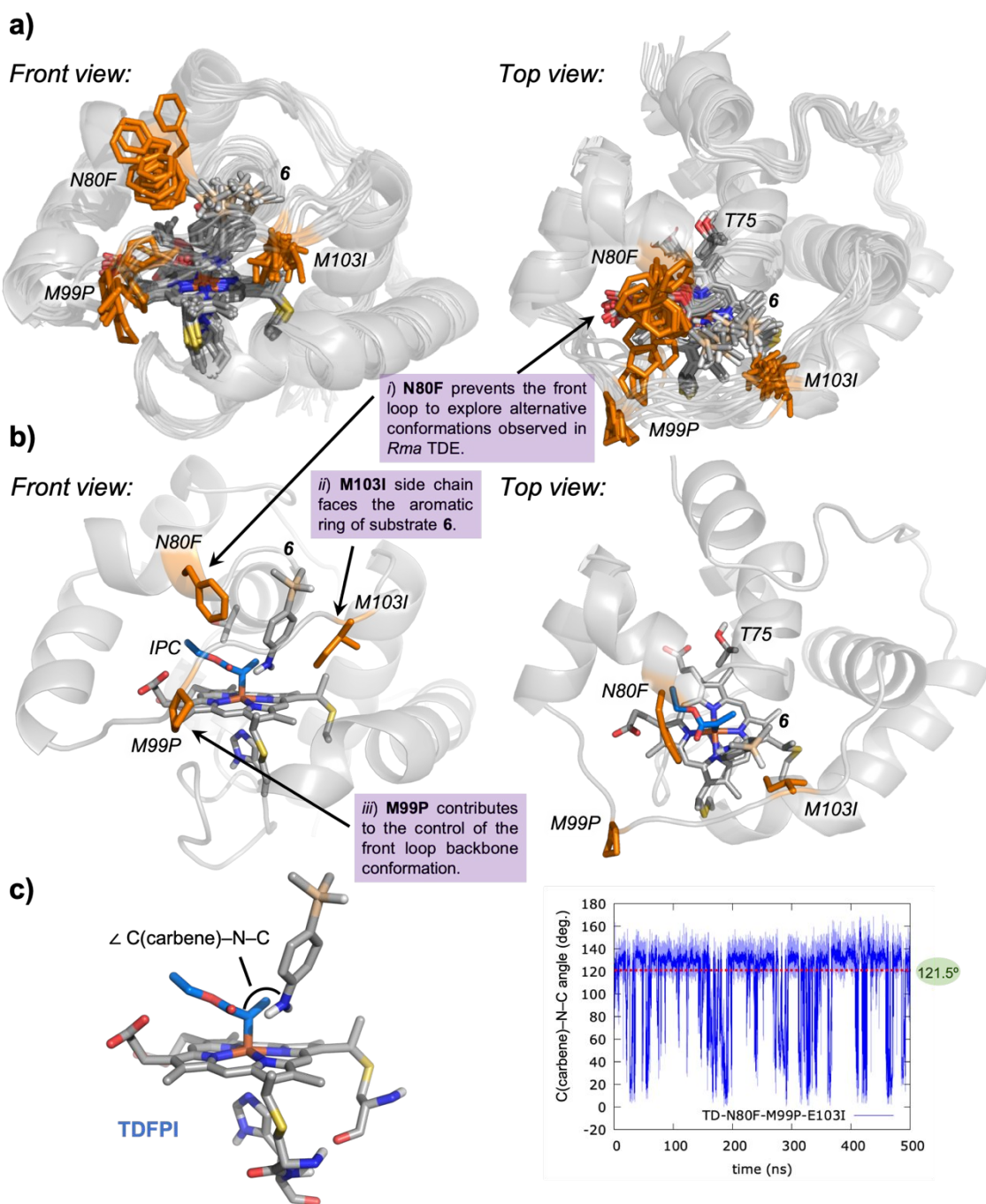


Figure S11. Analysis of near attack conformations explored by substrate **6** in *Rma* TDFPI from constrained MD simulations. **a)** Overlay of representative snapshots obtained from constrained MD trajectory (500 ns) from two different views (front view and top view); and **b)** selected representative snapshots to show the main near attack conformation adopted by substrate **6** during the simulations. **c)** C(carbene)-N(silane)-C(silane) attack angle explored along the constrained MD simulations. The ideal C(carbene)-N(silane)-C(silane) attack angle value for an effective *N*-nucleophilic attack is 121.5°, measured from DFT optimized TS (shown in **Figure 3b** in the main text).



Simulations revealed that silane **6** is highly stabilized in a near attack conformation that leads to the effective *N*-nucleophilic attack to the carbene, mainly due to hydrophobic interactions between the silane aryl ring and M103I residue, and the front loop conformation promoted by the M99P mutation. When **6** is bound, the N80F side chain mainly explores a conformation that sterically pushes the front loop to distance from the D-helix (where the N80F residue resides).

Table S1. Predicted KIE values from DFT and QM/MM optimized transition states (TS2) for carbene Si–H insertions.

Truncated DFT model	Computed KIE
TS2-CSS	1.488
TS2-T	2.726
QM/MM	Computed KIE
TDE-TS2-CSS	1.735
TDE-TS2-OSS	2.805
TDE-TS2-T	2.947

Table S2. DFT optimized structures. Energies and thermochemistry parameters (at T = 298.15 K and P = 1 atm) of all computationally characterized stationary points: Electronic energies (E), electronic energies from high level single point calculations (E (SP)), zero point energy (ZPE), enthalpy (H), entropic term (T·S), quasi-harmonic corrected entropic term (T·S-qh), free energy (G(T)), quasi-harmonic corrected free energy (G(T)- qh). All energies are given in a.u..

Structure	E	ZPE	H	T·S	T·S-qh	G(T)	G(T)-qh	E (SP)
1	-601.599814	0.169849	-601.418444	0.048127	0.046793	-601.466571	-601.465237	-601.786984527
8	-1002.789191	0.313235	-1002.454093	0.072956	0.067883	-1002.527049	-1002.521977	-1003.18067329
6	-656.957078	0.186107	-656.757985	0.051372	0.049630	-656.809357	-656.807615	-657.175687476
7	-1002.767085	0.311752	-1002.433797	0.073558	0.067627	-1002.507355	-1002.501424	-1003.14808201
3	-947.431705	0.297130	-947.114281	0.069027	0.064955	-947.183309	-947.179236	-947.791688120
2	-455.265588	0.130489	-455.123787	0.047900	0.046952	-455.171687	-455.170739	-455.475721644
TS2-CSS	-2285.914894	0.633168	-2285.237667	0.118729	0.110053	-2285.356396	-2285.347720	-3426.74469549
TS2-T	-2285.897188	0.630506	-2285.221528	0.124966	0.113283	-2285.346495	-2285.334811	-3426.71997476
TS2-CSS (substrate 6)	-2341.271783	0.649387	-2340.576843	0.122137	0.112578	-2340.698980	-2340.689421	-3482.13328055
TS2-T (substrate 6)	-2341.252296	0.646674	-2340.559007	0.127295	0.115948	-2340.686302	-2340.674954	-3482.10759730
TS N-H HAT (substrate 6)	-2341.234494	0.645489	-2340.542965	0.126264	0.113685	-2340.669230	-2340.656650	-3482.08584525
TS N-nucleophilic attack (substrate 6)	-2341.290962	0.651090	-2340.594367	0.124502	0.112600	-2340.718868	-2340.706967	-3482.14064706
5-CSS	-1684.343369	0.462774	-1683.847495	0.096150	0.089601	-1683.943645	-1683.937095	-2824.95294655
5-OSS	-1684.346119	0.462504	-1683.850386	0.096903	0.089784	-1683.947289	-1683.940170	-2824.95422900
5-T	-1684.331005	0.461976	-1683.835636	0.098824	0.091178	-1683.934460	-1683.926814	-2824.93686799
TS1-OSS	-1793.823114	0.470353	-1793.317930	0.100004	0.092650	-1793.417933	-1793.410579	-2934.48643341
TS1-CSS	-1793.824462	0.470361	-1793.319168	0.098775	0.093054	-1793.417944	-1793.412223	-2934.49093108
TS1-T	-1793.819090	0.470061	-1793.313998	0.100390	0.094244	-1793.414387	-1793.408242	-2934.48171619
4-CSS	-1338.598792	0.340783	-1338.234437	0.074573	0.070792	-1338.309010	-1338.305229	-2479.02500103
4-Q	-1338.616376	0.337997	-1338.253676	0.080314	0.075221	-1338.333991	-1338.328898	-2479.02671722
4-T	-1338.611205	0.339465	-1338.247404	0.079059	0.073801	-1338.326463	-1338.321205	-2479.03164630
4-OSS	-1338.603317	0.340217	-1338.239215	0.075507	0.071614	-1338.314722	-1338.310829	-2479.02586007
N2	-109.521007	0.005473	-109.512230	0.021754	0.021754	-109.533983	-109.533983	-109.573727877
INT1-Carbenoid radical	-1684.986844	0.486741	-1684.467843	0.094206	0.088575	-1684.562049	-1684.556418	-2825.597972650
INT1-Silane radical	-600.940991	0.164754	-600.765014	0.048102	0.047130	-600.813117	-600.812144	-601.134048586
TS3-T	-2285.923180	0.649484	-2285.228543	0.128709	0.113560	-2285.357252	-2285.342103	-3426.740143120

N	2.12589	-0.60373	1.14411	H	-7.13544	1.41440	-1.22914
N	-0.43876	0.52963	1.68110	H	-1.37146	-1.27438	-0.11658
N	2.13261	0.67553	-1.43761	C	-2.71872	-3.57457	-1.00791
N	-0.45341	1.77226	-0.91180	H	-2.74627	-3.30011	-2.06754
C	3.38858	-0.96481	0.74785	H	-1.84008	-4.20255	-0.83300
C	-1.61129	1.23394	1.79985	H	-3.61380	-4.17478	-0.79959
C	1.96902	-1.10046	2.41278	C	-2.76074	-2.60659	1.94662
C	-0.24081	-0.08790	2.89154	H	-1.87548	-3.21077	2.16420
C	3.39153	0.13282	-1.47860	H	-2.76340	-1.75127	2.62810
C	-1.64740	2.26684	-0.45571	H	-3.65632	-3.21119	2.13874
C	1.97366	1.36116	-2.61530				
C	-0.27262	2.30803	-2.16223				
C	4.03948	-1.73502	1.78776				
C	-2.17149	1.05488	3.12288	3			
C	3.15510	-1.82235	2.82089	C	-2.30692	0.14671	-0.92423
C	-1.32065	0.23359	3.80041	C	-1.44599	0.16351	0.19067
C	4.04317	0.47398	-2.72654	C	-1.53554	-0.91420	1.09236
C	-2.25559	3.11756	-1.45796	C	-2.43470	-1.96366	0.88884
C	3.16156	1.23249	-3.43438	C	-3.27256	-1.95889	-0.22818
C	-1.40172	3.14286	-2.51842	C	-3.20765	-0.89915	-1.13536
H	5.04326	-2.13753	1.72350	H	-2.28248	0.96416	-1.64137
H	-3.09058	1.51012	3.47136	H	-0.89742	-0.93784	1.97257
H	3.28287	-2.31248	3.77848	H	-2.48387	-2.78124	1.60368
H	-1.39789	-0.12563	4.81956	H	-3.86021	-0.88521	-2.00470
H	5.04466	0.16838	-3.00428	Si	-0.21857	1.57678	0.46741
H	-3.20555	3.62508	-1.34379	C	-1.00543	3.22399	-0.02920
H	3.28974	1.68079	-4.41219	H	-0.28272	4.04276	0.07144
H	-1.50411	3.67846	-3.45453	H	-1.36995	3.22782	-1.06220
C	3.97846	-0.62579	-0.46853	H	-1.85721	3.44909	0.62347
C	-2.18563	2.02295	0.80512	C	0.31190	1.64363	2.27779
C	0.84974	2.10931	-2.96461	H	0.88302	0.75824	2.57479
C	0.86020	-0.87439	3.22567	H	0.95362	2.51576	2.45052
H	4.99173	-0.97844	-0.64185	H	-0.55787	1.73168	2.93926
H	-3.13492	2.49648	1.03774	C	1.35703	1.34061	-0.63966
H	0.86257	2.60183	-3.93312	H	1.98248	2.20510	-0.38106
H	0.87448	-1.31123	4.22049	C	2.14323	0.13893	-0.18585
C	2.16878	2.39259	2.16794	O	2.92812	0.13782	0.74858
C	2.02863	3.45171	0.28977	O	1.86362	-0.96491	-0.91619
C	2.62970	4.31277	1.16944	C	2.56398	-2.18429	-0.56571
N	1.74497	2.25682	0.92249	H	2.56767	-2.76531	-1.49102
N	2.71046	3.62173	2.36156	H	3.59163	-1.93284	-0.29313
H	2.99689	5.32156	1.06268	C	1.86196	-2.93417	0.55588
H	1.78175	3.60525	-0.74877	H	1.89447	-2.35847	1.48517
H	2.10081	1.64242	2.94014	H	0.81630	-3.12974	0.29815
H	3.10319	3.96438	3.22689	H	2.36267	-3.89398	0.72754
C	0.02278	-1.04947	-0.78742	C	1.03390	1.36177	-2.14582
C	0.57988	-2.40157	-0.41919	H	0.57321	2.31523	-2.42438
O	0.23767	-3.11879	0.50730	H	1.94124	1.24372	-2.74945
O	1.55350	-2.75274	-1.28873	H	0.34655	0.55756	-2.42267
C	2.26064	-3.98265	-1.00103	H	-3.97429	-2.77330	-0.38861
H	1.53351	-4.79610	-0.91835				
H	2.76292	-3.87525	-0.03498				
C	3.24766	-4.21579	-2.12935				
H	3.80840	-5.13868	-1.94424	TS1-OSS			
H	2.73031	-4.31410	-3.08950	Fe	-0.32395	0.02206	0.03277
H	3.95787	-3.38617	-2.20160	N	-0.87478	-1.90845	-0.03878
C	-0.44343	-1.01499	-2.23249	N	-2.03428	0.58159	-0.87497
H	-0.86287	-1.96265	-2.58992	N	1.30743	-0.52169	1.11309
H	-1.16212	-0.21051	-2.39540	N	0.14891	1.97923	0.26712
H	0.43496	-0.79487	-2.84975	C	-0.17975	-3.00299	0.42314
Si	-2.71161	-2.07856	0.14434	C	-2.44783	1.85696	-1.18697
C	-4.13491	-0.92316	-0.30035	C	-2.04258	-2.39834	-0.56885
C	-4.98824	-0.40235	0.69132	C	-3.04744	-0.25318	-1.27645
C	-4.40081	-0.57224	-1.63895	C	1.69866	-1.79080	1.46022
C	-6.06186	0.42870	0.36280	C	-0.53790	3.07159	-0.20374
H	-4.81581	-0.64722	1.73613	C	2.23041	0.32752	1.67094
C	-5.46685	0.26479	-1.97306	C	1.25427	2.47413	0.91442
H	-3.76944	-0.95581	-2.43716	C	-0.91942	-4.21291	0.15567
C	-6.30175	0.76642	-0.97115	C	-3.74483	1.82001	-1.82144
H	-6.71007	0.81198	1.14692	C	-2.07752	-3.83782	-0.45439
H	-5.64831	0.52212	-3.01343	C	-4.11911	0.51184	-1.87143

C	-2.67638	-0.75194	1.00362
C	-3.51150	-0.40512	-0.07416
C	-3.04975	0.55924	-0.98865
H	-1.48779	1.89104	-1.55402
H	-0.81810	-0.45100	2.00108
H	-3.01681	-1.48840	1.72867
H	-3.68234	0.84835	-1.82539
Si	0.75280	1.59858	0.44844
C	0.69787	3.41976	-0.06608
H	1.69799	3.86755	-0.01867
H	0.31791	3.56302	-1.08361
H	0.04713	3.98439	0.61215
C	1.33837	1.46736	2.23970
H	1.50342	0.42972	2.54719
H	2.28970	1.99754	2.36713
H	0.60951	1.91777	2.92368
N	-4.78708	-0.95252	-0.19606
H	-5.17015	-0.94557	-1.13391
H	-4.91221	-1.85505	0.24680
C	2.06810	0.73725	-0.69345
H	2.99655	1.28036	-0.47353
C	2.31955	-0.67228	-0.23072
O	3.06778	-0.97881	0.68364
O	1.59591	-1.58056	-0.92648
C	1.76122	-2.97367	-0.56597
H	1.50214	-3.51819	-1.47728
H	2.81194	-3.15272	-0.32569
C	0.85558	-3.36926	0.59028
H	1.14565	-2.84506	1.50511
H	-0.18924	-3.13310	0.36520
H	0.93725	-4.44745	0.77036
C	1.72671	0.86801	-2.18983
H	1.68269	1.92280	-2.48072
H	2.48412	0.38306	-2.81681
H	0.76166	0.41004	-2.42431

TS2-T (substrate 6)

Fe	-1.07958	-0.55524	0.04438
N	-2.73205	0.39685	0.70121
N	-0.21611	-0.37193	1.85907
N	-2.02528	-0.89933	-1.70984
N	0.50469	-1.64870	-0.56467
C	-3.86129	0.71567	-0.01511
C	1.03198	-0.79733	2.24006
C	-2.94365	0.86379	1.97510
C	-0.78033	0.19732	2.97134
C	-3.24212	-0.41088	-2.11855
C	1.67120	-1.88505	0.11968
C	-1.54734	-1.65169	-2.75338
C	0.63348	-2.29075	-1.77111
C	-4.80252	1.41768	0.82456
C	1.26375	-0.48525	3.63210
C	-4.23689	1.49983	2.06222
C	0.13510	0.12752	4.08705
C	-3.53673	-0.85989	-3.45922
C	2.56764	-2.68377	-0.68168
C	-2.48882	-1.63824	-3.84942
C	1.91997	-2.94301	-1.85224
H	-5.77023	1.77835	0.49879
H	2.17158	-0.71882	4.17440
H	-4.64249	1.94891	2.96030
H	-0.07390	0.50605	5.07990
H	-4.43605	-0.61240	-4.00929
H	3.55745	-2.99486	-0.37297
H	-2.34777	-2.15803	-4.78899
H	2.26734	-3.51578	-2.70325
C	-4.09670	0.36320	-1.33981
C	1.93032	-1.47882	1.42501

C	-0.32303	-2.31206	-2.78230
C	-2.05133	0.75863	3.03595
H	-5.03478	0.68009	-1.78545
H	2.89483	-1.74052	1.84801
H	-0.08083	-2.86915	-3.68260
H	-2.36332	1.17393	3.98959
C	-1.37767	-3.37510	1.46942
C	-3.28710	-2.87482	0.58385
C	-3.45181	-4.09320	1.18712
N	-1.99032	-2.43709	0.76645
N	-2.22546	-4.39581	1.74522
H	-4.30023	-4.75436	1.27000
H	-4.00405	-2.28454	0.03467
H	-0.34718	-3.34996	1.78848
H	-1.99619	-5.22912	2.26900
C	-0.22181	1.15916	-0.67502
C	-0.85212	2.40486	-0.16359
O	-0.71408	2.88101	0.95622
O	-1.60492	3.04982	-1.10875
C	-2.24990	4.26806	-0.68995
H	-1.49238	4.97065	-0.32617
H	-2.92491	4.04682	0.14361
C	-3.00186	4.82346	-1.88686
H	-3.50822	5.75530	-1.61097
H	-2.31753	5.03570	-2.71515
H	-3.75645	4.11139	-2.23738
C	0.07855	1.19269	-2.16676
H	0.61008	2.11416	-2.44070
H	0.70550	0.34511	-2.45698
H	-0.83403	1.16181	-2.77090
Si	2.62646	2.11693	0.24010
C	4.17594	1.09122	-0.09258
C	4.98499	0.59322	0.94887
C	4.57634	0.75562	-1.40288
C	6.11724	-0.18283	0.70850
H	4.73079	0.81842	1.98234
C	5.70401	-0.01798	-1.66301
H	3.99092	1.10454	-2.25172
C	6.49801	-0.50237	-0.60701
H	6.72119	-0.53854	1.54135
H	5.98204	-0.24910	-2.68957
H	1.17381	1.33409	-0.10497
C	2.63327	3.63782	-0.90599
H	2.74620	3.36377	-1.96124
H	1.69727	4.20043	-0.80659
H	3.45922	4.31343	-0.64771
C	2.60994	2.72253	2.03665
H	1.71078	3.32652	2.19615
H	2.57590	1.89509	2.75300
H	3.49044	3.33889	2.26149
N	7.66776	-1.22439	-0.86239
H	7.96510	-1.83118	-0.10704
H	7.67582	-1.71722	-1.74795

TS N-H HAT

Fe	-1.19567	-0.45942	0.09420
N	-2.73086	0.52387	1.02279
N	-0.03243	-0.15857	1.68407
N	-2.47371	-0.92927	-1.43681
N	0.23757	-1.57968	-0.76465
C	-4.00438	0.72015	0.54595
C	1.26165	-0.58935	1.85476
C	-2.70072	1.08976	2.26881
C	-0.36249	0.51501	2.83947
C	-3.77200	-0.51298	-1.59179
C	1.49827	-1.81536	-0.27925
C	-2.19360	-1.71577	-2.52196
C	0.14761	-2.28506	-1.94334

C	-4.79460	1.44585	1.51639				
C	1.76642	-0.16395	3.14078				
C	-3.98376	1.67430	2.58817				
C	0.75915	0.51938	3.75105				
C	-4.32332	-1.04254	-2.82002				
C	2.23624	-2.66725	-1.18554				
C	-3.34326	-1.79304	-3.39638				
C	1.39659	-2.96163	-2.21610				
H	-5.83249	1.72573	1.38346				
H	2.76221	-0.37270	3.51074				
H	-4.21787	2.18348	3.51490				
H	0.75615	0.98637	4.72820				
H	-5.33077	-0.86094	-3.17377				
H	3.25766	-2.99233	-1.03234				
H	-3.37887	-2.35321	-4.32266				
H	1.58576	-3.58007	-3.08488				
C	-4.48614	0.25778	-0.67601				
C	1.98460	-1.34558	0.93804				
C	-0.97683	-2.35373	-2.75861				
C	-1.59519	1.09326	3.11586				
H	-5.51699	0.49398	-0.92476				
H	3.00506	-1.60497	1.20179				
H	-0.89842	-2.95296	-3.66134				
H	-1.70650	1.58620	4.07737				
C	-3.20487	-2.63620	1.12280				
C	-1.18910	-3.20047	1.66998				
C	-2.00732	-4.18821	2.14969				
N	-1.94678	-2.23745	1.03135				
N	-3.28601	-3.81198	1.79221				
H	-1.80510	-5.09635	2.69560				
H	-0.11622	-3.11472	1.73796				
H	-4.06138	-2.11420	0.72656				
H	-4.13688	-4.31958	1.99022				
C	-0.72862	1.20744	-0.96272				
C	-1.38057	2.47612	-0.48666				
O	-1.00954	3.14355	0.46902				
O	-2.42679	2.84717	-1.25771				
C	-3.13877	4.03621	-0.84750				
H	-2.43141	4.86925	-0.79066				
H	-3.54894	3.87053	0.15353				
C	-4.23086	4.29007	-1.87021				
H	-4.79376	5.18890	-1.59534				
H	-3.80582	4.44167	-2.86789				
H	-4.92696	3.44618	-1.91498				
C	-0.59903	1.16285	-2.47320				
H	-0.08396	2.06192	-2.83574				
H	-0.03606	0.28570	-2.79580				
H	-1.58653	1.14040	-2.94300				
C	2.76218	1.73753	-0.35554				
C	3.47782	1.91779	0.85742				
C	3.42539	1.05493	-1.41047				
C	4.79511	1.49022	0.97876				
H	2.98669	2.42019	1.68710				
C	4.72900	0.60787	-1.26074				
H	2.88934	0.90556	-2.34353				
C	5.46051	0.81989	-0.06871				
H	5.31732	1.67227	1.91613				
H	5.19770	0.09218	-2.09739				
H	0.42762	1.27963	-0.53111				
N	1.51961	2.27633	-0.57992				
H	1.17455	2.75427	0.25824				
Si	7.24631	0.24934	0.11107				
H	7.62466	0.48316	1.53899				
C	8.40880	1.24991	-0.99870				
H	9.44778	0.92165	-0.87225				
H	8.14658	1.13043	-2.05691				
H	8.36103	2.31886	-0.76175				
C	7.41308	-1.59627	-0.27700				
H	8.45339	-1.92590	-0.16743				
H	6.79519	-2.20204	0.39581				
H	7.10206	-1.81614	-1.30566				
				7			
				C	-1.19694	-1.80062	-0.57082
				C	-0.01444	-1.06386	-0.35009
				C	-0.14332	0.28903	0.01489
				C	-1.40600	0.85993	0.16718
				C	-2.59521	0.13885	-0.04338
				C	-2.44604	-1.20954	-0.42642
				H	-1.12424	-2.84838	-0.85757
				H	0.73954	0.90290	0.14394
				H	-1.45858	1.90942	0.45060
				H	-3.32558	-1.82482	-0.61032
				C	2.44353	-1.39756	0.18055
				H	3.10394	-2.25301	-0.00176
				C	3.19483	-0.19734	-0.41603
				O	2.78017	0.54814	-1.27743
				O	4.41579	-0.09802	0.14921
				C	5.26853	0.98876	-0.30083
				H	6.28228	0.62509	-0.11970
				H	5.12028	1.12779	-1.37392
				C	4.98717	2.26760	0.47158
				H	3.97325	2.62681	0.27305
				H	5.10215	2.10670	1.54841
				H	5.69335	3.04654	0.16291
				C	2.28047	-1.26907	1.71077
				H	1.83119	-2.18600	2.10463
				H	3.25415	-1.12377	2.18470
				H	1.63294	-0.43043	1.97934
				N	1.21498	-1.69394	-0.54958
				H	1.11443	-2.68454	-0.72861
				Si	-4.28384	0.93313	0.18099
				H	-4.03722	2.37776	0.48278
				C	-5.32647	0.80559	-1.39367
				H	-5.50586	-0.24125	-1.66788
				H	-6.30346	1.28488	-1.25707
				H	-4.82751	1.29065	-2.24025
				C	-5.22741	0.16644	1.63299
				H	-4.66950	0.27428	2.57018
				H	-6.20445	0.64725	1.76450
				H	-5.40217	-0.90421	1.47074
				6			
				C	-0.62725	1.31516	-0.00196
				C	0.23238	0.20012	0.00137
				C	-0.38487	-1.06722	0.00777
				C	-1.76764	-1.21835	0.01073
				C	-2.60924	-0.08996	0.00817
				C	-2.01375	1.18379	0.00060
				H	-0.20579	2.31847	-0.00960
				H	0.22575	-1.96896	0.00779
				H	-2.20845	-2.21310	0.01777
				H	-2.64543	2.06976	-0.00079
				Si	2.10167	0.39959	-0.00415
				H	2.36944	1.87187	-0.01183
				C	2.88802	-0.35222	1.54519
				H	3.97626	-0.21543	1.53858
				H	2.49469	0.11435	2.45550
				H	2.68860	-1.42885	1.61000
				C	2.88055	-0.36577	-1.55092
				H	2.48337	0.09310	-2.46352
				H	3.96882	-0.22911	-1.55046
				H	2.68089	-1.44293	-1.60555
				N	-3.99484	-0.23363	0.07348
				H	-4.52485	0.55109	-0.28691
				H	-4.35185	-1.11238	-0.28290

TS N-nucleophilic attack

Fe	-1.54083	-0.27522	-0.04758
N	-2.50208	1.42969	0.51123
N	-1.29752	-0.74133	1.91311
N	-2.00392	0.08096	-1.99154
N	-0.77572	-2.07629	-0.58706
C	-3.11052	2.32954	-0.32578
C	-0.78396	-1.91010	2.41578
C	-2.68758	1.90563	1.78390
C	-1.63743	0.02292	3.00108
C	-2.66364	1.17927	-2.48144
C	-0.31337	-3.05256	0.25781
C	-1.69747	-0.69787	-3.07785
C	-0.63381	-2.57546	-1.85840
C	-3.68775	3.41478	0.44004
C	-0.77629	-1.87428	3.86396
C	-3.42217	3.15311	1.75064
C	-1.30278	-0.67239	4.22665
C	-2.77092	1.09544	-3.92330
C	0.16309	-4.19121	-0.50190
C	-2.16978	-0.06909	-4.29387
C	-0.03396	-3.89332	-1.81608
H	-4.22840	4.25217	0.01588
H	-0.41682	-2.67369	4.50034
H	-3.70106	3.73028	2.62384
H	-1.46898	-0.28217	5.22331
H	-3.25030	1.83641	-4.55137
H	0.57790	-5.09366	-0.06960
H	-2.05454	-0.48192	-5.28869
H	0.18633	-4.50090	-2.68538
C	-3.17861	2.22135	-1.71296
C	-0.31675	-2.98041	1.65174
C	-1.05065	-1.93242	-3.02274
C	-2.26936	1.26265	2.94730
H	-3.69076	3.01837	-2.24527
H	0.07264	-3.83910	2.19172
H	-0.87671	-2.44560	-3.96447
H	-2.48218	1.75416	3.89245
C	-3.99620	-2.10671	-0.78532
C	-4.42656	-1.14300	1.09936
C	-5.51232	-1.92907	0.81633
N	-3.48638	-1.26088	0.09417
N	-5.22091	-2.53600	-0.38867
H	-6.43716	-2.10796	1.34231
H	-4.25532	-0.50397	1.95124
H	-3.52092	-2.42494	-1.70002
H	-5.81074	-3.18442	-0.89081
C	0.09508	0.63433	-0.27882
C	0.30486	1.94845	0.42740
O	0.62351	2.12252	1.59577
O	0.08047	2.97339	-0.42023
C	0.12591	4.30759	0.14582
H	1.11098	4.46420	0.59574
H	-0.62718	4.37397	0.93611
C	-0.14806	5.28725	-0.97932
H	-0.11783	6.31140	-0.59147
H	0.60267	5.19635	-1.77117
H	-1.13670	5.11069	-1.41445
C	0.97772	0.50367	-1.49053
H	1.97518	0.93787	-1.35737
H	1.07288	-0.53568	-1.80712
H	0.48869	1.05324	-2.30691
C	3.10671	-0.36746	0.80230
C	3.68764	-1.47409	0.15773
C	3.90232	0.76991	1.04062
C	5.02745	-1.44144	-0.22164
H	3.08159	-2.35529	-0.04057
C	5.23848	0.78251	0.65251
H	3.46097	1.63314	1.53189

C	5.84458	-0.31847	0.01281
H	5.44589	-2.31710	-0.71363
H	5.82153	1.67858	0.85956
N	1.75646	-0.37306	1.14456
H	1.45886	0.29402	1.85078
Si	7.65394	-0.29502	-0.50378
H	7.92022	-1.60742	-1.17054
C	8.80102	-0.12909	0.99356
H	9.85304	-0.12967	0.68301
H	8.61435	0.80619	1.53542
H	8.65656	-0.95644	1.69778
C	8.00073	1.09936	-1.73670
H	9.05427	1.10010	-2.04192
H	7.38776	0.99241	-2.63897
H	7.78057	2.08063	-1.29862
H	1.32367	-1.28317	1.24800

4-Q

Fe	0.01268	0.00024	-0.26600
N	-2.07627	0.00045	-0.56495
N	0.01463	2.05925	-0.62030
N	0.01431	-2.05877	-0.62121
N	2.10303	-0.00007	-0.52862
C	-2.88217	-1.10400	-0.65853
C	1.12205	2.86995	-0.64600
C	-2.88197	1.10508	-0.65828
C	-1.09189	2.87037	-0.66775
C	-1.09241	-2.86962	-0.66865
C	2.91073	1.10411	-0.60215
C	1.12151	-2.86974	-0.64716
C	2.91057	-1.10433	-0.60268
C	-4.26713	-0.68148	-0.77767
C	0.69967	4.25186	-0.71318
C	-4.26700	0.68283	-0.77753
C	-0.66773	4.25213	-0.72675
C	-0.66860	-4.25149	-0.72796
C	4.29837	0.68178	-0.68972
C	0.69881	-4.25153	-0.71460
C	4.29827	-0.68217	-0.69005
H	-5.11580	-1.34841	-0.87054
H	1.36618	5.10489	-0.75268
H	-5.11554	1.34993	-0.87028
H	-1.33295	5.10548	-0.77956
H	-1.33402	-5.10467	-0.78083
H	5.14884	1.34899	-0.76126
H	1.36512	-5.10471	-0.75436
H	5.14863	-1.34947	-0.76193
C	-2.42483	-2.42740	-0.67759
C	2.45434	2.42745	-0.62931
C	2.45391	-2.42757	-0.63039
C	-2.42439	2.42840	-0.67696
H	-3.18569	-3.20120	-0.74011
H	3.21645	3.20116	-0.67453
H	3.21585	-3.20143	-0.67592
H	-3.18511	3.20236	-0.73940
C	-1.10934	-0.00137	2.69657
C	1.05274	-0.00077	2.81020
C	0.59997	-0.00122	4.10265
N	-0.02177	-0.00088	1.94107
N	-0.77777	-0.00161	4.00966
H	1.11122	-0.00129	5.05254
H	2.06713	-0.00036	2.44084
H	-2.12545	-0.00163	2.33211
H	-1.42850	-0.00206	4.78318

4-T
 Fe 0.01479 0.00012 -0.45177
 N -1.41613 -1.42116 -0.60948
 N -1.41543 1.42206 -0.60929
 N 1.44694 -1.42175 -0.57716
 N 1.44763 1.42130 -0.57701
 C -1.22267 -2.78260 -0.60718
 C -1.22134 2.78340 -0.60684
 C -2.77893 -1.23534 -0.67220
 C -2.77832 1.23690 -0.67216
 C 1.25320 -2.78300 -0.58002
 C 1.25454 2.78264 -0.57937
 C 2.81062 -1.23638 -0.61007
 C 2.81121 1.23528 -0.60976
 C -2.49256 -3.46917 -0.66358
 C -2.49089 3.47059 -0.66331
 C -3.45875 -2.50924 -0.70556
 C -3.45753 2.51113 -0.70552
 C 2.52388 -3.47011 -0.60948
 C 2.52555 3.46915 -0.60837
 C 3.49077 -2.51050 -0.62995
 C 3.49198 2.50907 -0.62908
 H -2.61192 -4.54559 -0.67729
 H -2.60973 4.54708 -0.67693
 H -4.53294 -2.63530 -0.76104
 H -4.53165 2.63772 -0.76114
 H 2.64312 -4.54657 -0.62076
 H 2.64534 4.54554 -0.61919
 H 4.56589 -2.63656 -0.66153
 H 4.56717 2.63462 -0.66045
 C 0.01506 -3.41858 -0.57768
 C 0.01669 3.41880 -0.57705
 C 3.45015 -0.00071 -0.62030
 C -3.41755 0.00094 -0.69580
 H 0.01491 -4.50478 -0.58073
 H 0.01704 4.50500 -0.57979
 H 4.53596 -0.00096 -0.64565
 H -4.50258 0.00120 -0.74515
 C -1.11052 -0.00032 2.63795
 C 1.04394 -0.00057 2.76435
 C 0.58727 -0.00105 4.05690
 N -0.02256 -0.00009 1.88799
 N -0.78976 -0.00085 3.95751
 H 1.09398 -0.00152 5.00949
 H 2.06200 -0.00053 2.40331
 H -2.12667 -0.00001 2.27185
 H -1.44428 -0.00106 4.72754

4-CSS
 Fe 0.00709 -0.00001 -0.38257
 N -1.41680 -1.42300 -0.54341
 N -1.41932 1.42051 -0.54338
 N 1.43419 -1.42039 -0.52749
 N 1.43169 1.42286 -0.52757
 C -1.22679 -2.78605 -0.54734
 C -1.23166 2.78391 -0.54694
 C -2.78053 -1.23935 -0.59042
 C -2.78275 1.23455 -0.59013
 C 1.24679 -2.78372 -0.53373
 C 1.24192 2.78584 -0.53423
 C 2.79755 -1.23426 -0.56301
 C 2.79536 1.23905 -0.56334
 C -2.49742 -3.47422 -0.59737
 C -2.50348 3.46990 -0.59644
 C -3.46236 -2.51392 -0.62532
 C -3.46678 2.50793 -0.62442
 C 2.51920 -3.46970 -0.57231
 C 2.51314 3.47401 -0.57338

C 3.48222 -2.50758 -0.59212
 C 3.47782 2.51355 -0.59308
 H -2.61620 -4.55062 -0.61858
 H -2.62416 4.54609 -0.61729
 H -4.53722 -2.63860 -0.67409
 H -4.54187 2.63078 -0.67282
 H 2.64019 -4.54587 -0.59196
 H 2.63223 4.55038 -0.59345
 H 4.55773 -2.62993 -0.63072
 H 4.55310 2.63775 -0.63203
 C 0.01061 -3.42125 -0.52642
 C 0.00465 3.42124 -0.52648
 C 3.43447 0.00296 -0.57097
 C -3.41959 -0.00298 -0.60235
 H 0.01166 -4.50766 -0.53268
 H 0.00383 4.50765 -0.53276
 H 4.52051 0.00391 -0.59897
 H -4.50541 -0.00394 -0.63929
 C -1.08512 -0.00037 2.35982
 C 1.08499 0.00037 2.43245
 C 0.65357 0.00037 3.73181
 N -0.00866 0.00003 1.58719
 N -0.72428 -0.00021 3.65673
 H 1.18557 0.00068 4.66995
 H 2.09100 0.00078 2.04408
 H -2.10672 -0.00092 2.01423
 H -1.36098 -0.00052 4.45010

4-OSS
 N -1.65974 -1.31694 0.20891
 N 1.04326 -1.74899 -0.63140
 N -1.48170 1.40345 -0.61474
 C -3.47697 0.33073 0.33419
 C -0.43163 -3.43879 0.37016
 C 3.00138 -0.70452 -1.68261
 C -0.00199 3.09704 -1.60348
 C -2.94867 -0.94507 0.51496
 C 0.77351 -3.02257 -0.18906
 C 2.48103 0.57724 -1.84106
 C -1.21605 2.67383 -1.06923
 C -3.68234 -2.06823 1.05381
 C 1.91508 -3.88303 -0.40714
 C 3.19441 1.68398 -2.43828
 C -2.38715 3.51106 -0.93480
 C -2.82305 -3.12522 1.06971
 C 2.87848 -3.11706 -0.99063
 C 2.35168 2.75369 -2.40919
 C -3.36719 2.73266 -0.39676
 C -1.56533 -2.64840 0.53923
 C 2.32587 -1.78791 -1.12698
 C 1.12296 2.29993 -1.79647
 C -2.79378 1.42005 -0.20060
 N 1.22104 0.97182 -1.45463
 H -4.51335 0.48539 0.62115
 H -0.50312 -4.47893 0.67573
 H 4.01492 -0.87690 -2.03372
 H 0.06421 4.13316 -1.92354
 H -4.71929 -2.03739 1.36507
 H -4.38821 3.00351 -0.15740
 H -2.43866 4.55260 -1.22757
 H 2.52619 3.75917 -2.77212
 H 4.20286 1.63028 -2.82968
 H 1.95392 -4.93461 -0.15060
 H 3.87066 -3.40997 -1.31133
 H -3.00989 -4.14059 1.39728
 Fe -0.16610 -0.13111 -0.47499
 N 0.51452 0.39974 1.43428
 C -0.24117 0.76265 2.45817

C	1.82108	0.43859	1.88018
H	-1.31773	0.83793	2.44854
C	1.84638	0.83120	3.19206
H	2.64082	0.18224	1.22680
H	0.18695	1.32983	4.44637
H	2.65557	0.98193	3.88924
N	0.52633	1.03253	3.54218

N2			
N	0.00000	-0.00000	0.55257
N	0.00000	-0.00000	-0.55257

2			
C	-1.21052	0.44179	0.00008
C	-0.06615	-0.46940	0.00005
O	-0.13087	-1.68963	0.00013
O	1.08863	0.23312	-0.00013
C	2.30624	-0.55149	-0.00002
H	2.30854	-1.19605	-0.88443
H	2.30845	-1.19585	0.88452
C	3.47199	0.41839	-0.00003
H	4.41405	-0.14007	0.00019
H	3.45059	1.05728	-0.88875
H	3.45039	1.05758	0.88846
C	-1.13872	1.94963	0.00006
H	-0.60595	2.31363	0.88501
H	-0.60718	2.31387	-0.88556
H	-2.14222	2.38305	0.00085
N	-2.37833	-0.14811	-0.00004
N	-3.39536	-0.66258	-0.00013

1			
C	-1.11697	-1.25763	-0.00111
C	-0.22776	-0.16743	-0.00020
C	-0.78437	1.12649	0.00093
C	-2.16600	1.32406	0.00115
C	-3.02858	0.22456	0.00024
C	-2.50142	-1.06798	-0.00089
H	-0.72410	-2.27220	-0.00202
H	-0.13245	1.99853	0.00165
H	-2.57041	2.33322	0.00204
H	-4.10502	0.37566	0.00040
H	-3.16670	-1.92783	-0.00162
Si	1.64251	-0.43378	-0.00049
H	1.85684	-1.91340	-0.00218
C	2.43316	0.30519	-1.55164
H	3.51634	0.13397	-1.55663
H	2.01671	-0.14240	-2.46111
H	2.26674	1.38781	-1.60567
C	2.43313	0.30160	1.55239
H	2.01672	-0.14810	2.46083
H	3.51633	0.13037	1.55697
H	2.26672	1.38409	1.60892

INT1-Silane radical			
Si	-1.66143	-0.00019	-0.41866
C	0.19979	-0.00004	-0.16005
C	0.93035	-1.20576	-0.08726
C	0.93013	1.20577	-0.08647
C	2.31710	-1.20789	0.06601
H	0.40897	-2.15853	-0.14578
C	2.31689	1.20804	0.06680

H	0.40858	2.15848	-0.14434
C	3.01614	0.00011	0.14439
H	2.85332	-2.15175	0.12620
H	2.85294	2.15196	0.12761
H	4.09643	0.00017	0.26321
C	-2.47606	1.56612	0.28238
H	-2.06257	2.47819	-0.16103
H	-3.55234	1.55642	0.07685
H	-2.34096	1.62721	1.37087
C	-2.47589	-1.56605	0.28361
H	-3.55222	-1.55656	0.07834
H	-2.06243	-2.47839	-0.15925
H	-2.34048	-1.62635	1.37210

INT1-Carbenoid radical			
Fe	-0.33346	0.00961	-0.07122
N	1.33029	-0.31320	1.04587
N	-0.65930	-1.96789	-0.17091
N	-0.08408	1.98714	0.15801
N	-2.06023	0.33521	-1.08262
C	2.19917	0.63006	1.53380
C	-1.64654	-2.60852	-0.88024
C	1.80235	-1.52561	1.48187
C	0.09271	-2.95561	0.41570
C	0.97713	2.62859	0.75298
C	-2.86372	-0.60891	-1.67078
C	-0.93883	2.97644	-0.26707
C	-2.64865	1.54732	-1.33868
C	3.25754	-0.00491	2.28923
C	-1.51215	-4.03777	-0.73788
C	3.00621	-1.34349	2.26343
C	-0.44011	-4.25233	0.07628
C	0.79231	4.05705	0.68944
C	-3.98852	0.02596	-2.32399
C	-0.40130	4.27239	0.06542
C	-3.86036	1.36408	-2.10870
H	4.06935	0.52073	2.77664
H	-2.16558	-4.76735	-1.19971
H	3.57178	-2.14569	2.72097
H	-0.02895	-5.19491	0.41528
H	1.48805	4.78692	1.08428
H	-4.76801	-0.50026	-2.86078
H	-0.88318	5.21553	-0.16042
H	-4.50998	2.16586	-2.43713
C	2.05226	2.00437	1.37967
C	-2.66166	-1.98358	-1.59997
C	-2.14021	2.78017	-0.94378
C	1.22045	-2.75732	1.20588
H	2.81393	2.64338	1.81655
H	-3.37476	-2.62232	-2.11244
H	-2.70838	3.66559	-1.21314
H	1.70670	-3.64107	1.60801
C	-1.01713	0.20436	3.02282
C	-2.85792	-0.16704	1.94871
C	-3.19595	-0.08978	3.27363
N	-1.49685	0.01773	1.80401
N	-2.01183	0.14868	3.94168
H	-4.13932	-0.17994	3.78911
H	-3.49186	-0.34177	1.09372
H	0.01761	0.38038	3.27131
H	-1.90061	0.26039	4.93991
C	0.64138	-0.07326	-1.90441
C	1.98339	-0.71121	-1.79085
O	2.20967	-1.91282	-1.83427
O	2.99474	0.19286	-1.66153
C	4.32203	-0.34958	-1.53449
H	4.52947	-0.99908	-2.39158
H	4.37055	-0.96481	-0.63021

C	5.29005	0.81856	-1.46761
H	6.31665	0.44832	-1.36899
H	5.23000	1.42955	-2.37460
H	5.06885	1.45775	-0.60635
C	0.65637	1.24370	-2.68401
H	1.08333	1.09119	-3.68754
H	-0.35715	1.62919	-2.81453
H	1.25437	2.01185	-2.18917
H	-0.00611	-0.79794	-2.40158

TS3-T

Fe	-1.35334	-0.33277	-0.02327
N	-2.24017	1.45811	0.24629
N	-0.99128	-0.43352	1.95931
N	-1.80403	-0.27952	-1.99028
N	-0.52112	-2.15982	-0.28549
C	-2.79964	2.24808	-0.72691
C	-0.31619	-1.43214	2.61653
C	-2.45303	2.11261	1.43587
C	-1.35111	0.47863	2.92116
C	-2.40733	0.75569	-2.66286
C	0.08442	-2.92508	0.67945
C	-1.56539	-1.25562	-2.93031
C	-0.45682	-2.89167	-1.44660
C	-3.36579	3.44077	-0.13821
C	-0.24763	-1.14098	4.03140
C	-3.15676	3.35298	1.20580
C	-0.89781	0.04117	4.22116
C	-2.54780	0.42656	-4.06257
C	0.55563	-4.16722	0.10942
C	-2.03127	-0.82441	-4.22724
C	0.21338	-4.14958	-1.20923
H	-3.86477	4.22566	-0.69327
H	0.23202	-1.77270	4.76885
H	-3.44480	4.05210	1.98103
H	-1.05780	0.58246	5.14526
H	-2.99160	1.07547	-4.80758
H	1.06943	-4.94423	0.66197
H	-1.96097	-1.41074	-5.13503
H	0.39210	-4.90627	-1.96304
C	-2.86173	1.93679	-2.08234
C	0.19990	-2.58238	2.02468
C	-0.95175	-2.47948	-2.68033
C	-2.05097	1.65656	2.68622
H	-3.33251	2.66345	-2.73823
H	0.70775	-3.28912	2.67461
H	-0.83095	-3.15817	-3.51961
H	-2.28026	2.28196	3.54388
C	-4.33356	-1.67367	-0.56285

C	-3.96373	-1.78471	1.56034
C	-5.20273	-2.33648	1.36068
N	-3.43064	-1.37508	0.35463
N	-5.42310	-2.25699	0.00077
H	-5.92678	-2.76542	2.03603
H	-3.41924	-1.65405	2.48331
H	-4.23961	-1.48758	-1.62193
H	-6.24697	-2.57441	-0.49084
C	0.83505	0.55824	-0.34841
C	0.77351	1.93870	0.15942
O	0.85353	2.28640	1.33370
O	0.61397	2.84705	-0.84457
C	0.50444	4.22712	-0.44863
H	1.40960	4.51857	0.09512
H	-0.34556	4.33728	0.23170
C	0.32085	5.05078	-1.71110
H	0.23734	6.11280	-1.45470
H	1.17212	4.92588	-2.38875
H	-0.58903	4.75026	-2.24095
C	1.24869	0.31725	-1.78576
H	2.26154	0.69239	-1.98336
H	1.24059	-0.75135	-2.01053
H	0.57786	0.82026	-2.48565
Si	3.93225	0.76536	0.93541
C	5.27592	-0.16516	0.01195
C	5.50697	-1.54003	0.23773
C	6.05097	0.46570	-0.98610
C	6.47125	-2.24402	-0.48379
H	4.92848	-2.06792	0.99233
C	7.01610	-0.23484	-1.70970
H	5.90226	1.52199	-1.19840
C	7.23081	-1.59371	-1.46087
H	6.63245	-3.30046	-0.28334
H	7.60274	0.27886	-2.46743
H	7.98202	-2.14108	-2.02416
H	1.17549	-0.15108	0.39731
C	4.29948	2.61781	1.08929
H	4.54433	3.07455	0.12442
H	3.41349	3.12226	1.48812
H	5.13901	2.79808	1.77435
C	3.52237	-0.00431	2.61584
H	2.64744	0.50236	3.03630
H	3.28023	-1.06907	2.53301
H	4.35832	0.10463	3.32002

V. Supplementary References:

1. Gibson, D. G.; Young, L.; Chuang, R.-Y.; Venter, J. C.; Hutchison III, C. A.; Smith, H. O., Enzymatic assembly of DNA molecules up to several hundred kilobases. *Nature Methods* **2009**, *6*, 343–345
2. Arslan, E.; Schulz, H.; Zufferey, R.; Künzler, P.; Thöny-Meyer, L., Overproduction of the *Bradyrhizobium japonicum* c-Type Cytochrome Subunits of the *cbb3* Oxidase in *Escherichia coli*. *Bioch. Bioph. Res. Comm.* **1998**, *251* (3), 744–747.
3. Sambrook, J.; Russell, D. W.; Russell, D. W., *Molecular cloning: a laboratory manual (3-volume set)*. Cold Spring Harbor Laboratory Press New York: 2001; Vol. 999.
4. M. J. Frisch, G. W. T., H. B. Schlegel, G. E. Scuseria, M. A. Robb, J. R. Cheeseman, G. Scalmani, V. Barone, G. A. Petersson, H. Nakatsuji, X. Li, M. Caricato, A. Marenich, J. Bloino, B. G. Janesko, R. Gomperts, B. Mennucci, H. P. Hratchian, J. V. Ortiz, A. F. Izmaylov, J. L. Sonnenberg, D. Williams-Young, F. Ding, F. Lipparini, F. Egidi, J. Goings, B. Peng, A. Petrone, T. Henderson, D. Ranasinghe, V. G. Zakrzewski, J. Gao, N. Rega, G. Zheng, W. Liang, M. Hada, M. Ehara, K. Toyota, R. Fukuda, J. Hasegawa, M. Ishida, T. Nakajima, Y. Honda, O. Kitao, H. Nakai, T. Vreven, K. Throssell, J. A. Montgomery, Jr., J. E. Peralta, F. Ogliaro, M. Bearpark, J. J. Heyd, E. Brothers, K. N. Kudin, V. N. Staroverov, T. Keith, R. Kobayashi, J. Normand, K. Raghavachari, A. Rendell, J. C. Burant, S. S. Iyengar, J. Tomasi, M. Cossi, J. M. Millam, M. Klene, C. Adamo, R. Cammi, J. W. Ochterski, R. L. Martin, K. Morokuma, O. Farkas, J. B. Foresman, and D. J. Fox, Gaussian 09, Revision A. 02. Gaussian, Inc.: Wallingford, CT **2009**.
5. Becke, A. D., Density-functional exchange-energy approximation with correct asymptotic behavior. *Phys. Rev. A* **1988**, *38* (6), 3098–3100.
6. Becke, A. D., Density-functional thermochemistry. III. The role of exact exchange. *J. Chem. Phys.* **1993**, *98* (7), 5648–5652.
7. Lee, C.; Yang, W.; Parr, R. G., Development of the Colle-Salvetti correlation-energy formula into a functional of the electron density. *Phys. Rev. B* **1988**, *37* (2), 785–789.
8. Ribeiro, R. F.; Marenich, A. V.; Cramer, C. J.; Truhlar, D. G., Use of Solution-Phase Vibrational Frequencies in Continuum Models for the Free Energy of Solvation. *J. Phys. Chem. B* **2011**, *115* (49), 14556–14562.
9. Zhao, Y.; Truhlar, D. G., Computational characterization and modeling of buckyball tweezers: density functional study of concave-convex $\pi \cdots \pi$ interactions. *Phys. Chem. Chem. Phys.* **2008**, *10* (19), 2813–2818.
10. Ignacio Funes-Ardoiz & Robert S. Paton. GoodVibes: GoodVibes v1.0.1. (2016). doi:10.5281/zenodo.60811
11. Grimme, S.; Ehrlich, S.; Goerigk, L., Effect of the damping function in dispersion corrected density functional theory. *J. Comput. Chem.* **2011**, *32* (7), 1456–1465.
12. Grimme, S.; Antony, J.; Ehrlich, S.; Krieg, H., A consistent and accurate ab initio parametrization of density functional dispersion correction (DFT-D) for the 94 elements H-Pu. *J. Chem. Phys.* **2010**, *132* (15), 154104.
13. Barone, V.; Cossi, M., Quantum Calculation of Molecular Energies and Energy Gradients in Solution by a Conductor Solvent Model. *J. Phys. Chem. A* **1998**, *102* (11), 1995–2001.
14. Cossi, M.; Rega, N.; Scalmani, G.; Barone, V., Energies, structures, and electronic properties of molecules in solution with the C-PCM solvation model. *J. Comput. Chem.* **2003**, *24* (6), 669–681.
15. Schutz, C. N.; Warshel, A., What are the dielectric “constants” of proteins and how to validate electrostatic models? *Proteins* **2001**, *44* (4), 400–417.
16. Li, L.; Li, C.; Zhang, Z.; Alexov, E., On the Dielectric “Constant” of Proteins: Smooth Dielectric Function for Macromolecular Modeling and Its Implementation in DelPhi. *J. Chem. Theory Comp.* **2013**, *9* (4), 2126–2136.
17. Sharon, D. A.; Mallick, D.; Wang, B.; Shaik, S., Computation Sheds Insight into Iron Porphyrin Carbenes’ Electronic Structure, Formation, and N–H Insertion Reactivity. *J. Am. Chem. Soc.* **2016**, *138* (30), 9597–9610.
18. Postils, V.; Rodriguez, M.; Sabenya, G.; Conde, A.; Diaz-Requejo, M. M.; Pérez, P. J.; Costas, M.; Solà, M.; Luis, J. M., The Mechanism of the Selective Fe-Catalyzed Arene Carbon-Hydrogen Bond Functionalization. *ACS Catal.* **2018**, *8* (5), 4313–4322.
19. Lewis, R. D.; Garcia-Borràs, M.; Chalkley, M. J.; Buller, A. R.; Houk, K. N.; Kan, S. B. J.; Arnold, F. H., Catalytic iron-carbene intermediate revealed in a cytochrome *c* carbene transferase. *Proc. Natl. Acad. Sci. USA* **2018**, *115* (28), 7308–7313.

20. Huang, X.; Garcia-Borràs, M.; Miao, K.; Kan, S. B. J.; Zutshi, A.; Houk, K. N.; Arnold, F. H., A Biocatalytic Platform for Synthesis of Chiral α -Trifluoromethylated Organoborons. *ACS Cent. Sci.* **2019**, *5* (2), 270–276.
21. Narayan, A. R. H.; Jiménez-Osés, G.; Liu, P.; Negretti, S.; Zhao, W.; Gilbert, M. M.; Ramabhadran, R. O.; Yang, Y.-F.; Furan, L. R.; Li, Z.; Podust, L. M.; Montgomery, J.; Houk, K. N.; Sherman, D. H., Enzymatic hydroxylation of an unactivated methylene C–H bond guided by molecular dynamics simulations. *Nat. Chem.* **2015**, *7*, 653–660.
22. Gilbert, M. M.; DeMars, M. D.; Yang, S.; Grandner, J. M.; Wang, S.; Wang, H.; Narayan, A. R. H.; Sherman, D. H.; Houk, K. N.; Montgomery, J., Synthesis of Diverse 11- and 12-Membered Macrolactones from a Common Linear Substrate Using a Single Biocatalyst. *ACS Cent. Sci.* **2017**, *3* (12), 1304–1310.
23. Shaik, S.; Cohen, S.; Wang, Y.; Chen, H.; Kumar, D.; Thiel, W., P450 Enzymes: Their Structure, Reactivity, and Selectivity—Modeled by QM/MM Calculations. *Chem. Rev.* **2010**, *110* (2), 949–1017.
24. Chen, H.; Lai, W.; Shaik, S., Exchange-Enhanced H-Abstraction Reactivity of High-Valent Nonheme Iron(IV)-Oxo from Coupled Cluster and Density Functional Theories. *J. Phys. Chem. Lett.* **2010**, *1* (10), 1533–1540.
25. Altun, A.; Breidung, J.; Neese, F.; Thiel, W., Correlated Ab Initio and Density Functional Studies on H₂ Activation by FeO⁺. *J. Chem. Theory Comp.* **2014**, *10* (9), 3807–3820.
26. Seeger, R.; Pople, J. A., Self-consistent molecular orbital methods. XVIII. Constraints and stability in Hartree–Fock theory. *J. Chem. Phys.* **1977**, *66* (7), 3045–3050.
27. Bauernschmitt, R.; Ahlrichs, R., Stability analysis for solutions of the closed shell Kohn–Sham equation. *J. Chem. Phys.* **1996**, *104* (22), 9047–9052.
28. Schlegel, H. B.; McDouall, J. J. W., Do You Have SCF Stability and Convergence Problems? In *Computational Advances in Organic Chemistry: Molecular Structure and Reactivity*, Ögretir, C.; Csizmadia, I. G., Eds. Springer Netherlands: Dordrecht, 1991; pp 167–185.
29. Legault, C., CYLview, 1.0 b, Université de Sherbrooke, Sherbrooke, Québec, Canada, 2009. URL <http://www.cylview.org> (accessed February 1, 2016).
30. Dapprich, S.; Komáromi, I.; Byun, K. S.; Morokuma, K.; Frisch, M. J., A new ONIOM implementation in Gaussian98. Part I. The calculation of energies, gradients, vibrational frequencies and electric field derivatives. *J. Mol. Struct. (THEOCHEM)* **1999**, *461-462*, 1–21.
31. Chung, L. W.; Sameera, W. M. C.; Ramozzi, R.; Page, A. J.; Hatanaka, M.; Petrova, G. P.; Harris, T. V.; Li, X.; Ke, Z.; Liu, F.; Li, H.-B.; Ding, L.; Morokuma, K., The ONIOM Method and Its Applications. *Chem. Rev.* **2015**, *115* (12), 5678–5796.
32. Vreven, T.; Byun, K. S.; Komáromi, I.; Dapprich, S.; Montgomery, J. A.; Morokuma, K.; Frisch, M. J., Combining Quantum Mechanics Methods with Molecular Mechanics Methods in ONIOM. *J. Chem. Theory Comp.* **2006**, *2* (3), 815–826.
33. Tao, P.; Schlegel, H. B., A toolkit to assist ONIOM calculations. *J. Comput. Chem.* **2010**, *31* (12), 2363–2369.
34. Salomon-Ferrer, R.; Götz, A. W.; Poole, D.; Le Grand, S.; Walker, R. C., Routine Microsecond Molecular Dynamics Simulations with AMBER on GPUs. 2. Explicit Solvent Particle Mesh Ewald. *J. Chem. Theory Comp.* **2013**, *9* (9), 3878–3888.
35. D.A. Case, D. S. C., T.E. Cheatham, III, T.A. Darden, R.E. Duke, T.J. Giese, H. Gohlke, A.W. Goetz, D. Greene, N. Homeyer, S. Izadi, A. Kovalenko, T.S. Lee, S. LeGrand, P. Li, C. Lin, J. Liu, T. Luchko, R. Luo, D. Mermelstein, K.M. Merz, G. Monard, H. Nguyen, I. Omelyan, A. Onufriev, F. Pan, R. Qi, D.R. Roe, A. Roitberg, C. Sagui, C.L. Simmerling, W.M. Botello-Smith, J. Swails, R.C. Walker, J. Wang, R.M. Wolf, X. Wu, L. Xiao, D.M. York and P.A. Kollman *AMBER 2017*, University of California, San Francisco, 2017.
36. Li, P.; Merz, K. M., MCPB.py: A Python Based Metal Center Parameter Builder. *J. Chem. Inf. Model.* **2016**, *56* (4), 599–604.
37. Wang, J.; Wolf, R. M.; Caldwell, J. W.; Kollman, P. A.; Case, D. A., Development and testing of a general amber force field. *J. Comput. Chem.* **2004**, *25* (9), 1157–1174.
38. Bayly, C. I.; Cieplak, P.; Cornell, W.; Kollman, P. A., A well-behaved electrostatic potential based method using charge restraints for deriving atomic charges: the RESP model. *J. Phys. Chem.* **1993**, *97* (40), 10269–10280.
39. Besler, B. H.; Merz, K. M.; Kollman, P. A., Atomic charges derived from semiempirical methods. *J. Comput. Chem.* **1990**, *11* (4), 431–439.
40. Singh, U. C.; Kollman, P. A., An approach to computing electrostatic charges for molecules. *J. Comput. Chem.* **1984**, *5* (2), 129–145.

41. Jorgensen, W. L.; Chandrasekhar, J.; Madura, J. D.; Impey, R. W.; Klein, M. L., Comparison of simple potential functions for simulating liquid water. *J. Chem. Phys.* **1983**, *79* (2), 926–935.
42. Maier, J. A.; Martinez, C.; Kasavajhala, K.; Wickstrom, L.; Hauser, K. E.; Simmerling, C., ff14SB: Improving the Accuracy of Protein Side Chain and Backbone Parameters from ff99SB. *J. Chem. Theory Comp.* **2015**, *11* (8), 3696–3713.
43. Darden, T.; York, D.; Pedersen, L., Particle mesh Ewald: An N·log(N) method for Ewald sums in large systems. *J. Chem. Phys.* **1993**, *98* (12), 10089–10092.
44. Roe, D. R.; Cheatham, T. E., PTRAJ and CPPTRAJ: Software for Processing and Analysis of Molecular Dynamics Trajectory Data. *J. Chem. Theory Comp.* **2013**, *9* (7), 3084–3095.
45. Kumar, S.; Rosenberg, J. M.; Bouzida, D.; Swendsen, R. H.; Kollman, P. A., Multidimensional free-energy calculations using the weighted histogram analysis method. *J. Comput. Chem.* **1995**, *16* (11), 1339–1350.
46. Roux, B., The calculation of the potential of mean force using computer simulations. *Comp. Phys. Comm.* **1995**, *91* (1), 275–282.
47. Grossfield, A., WHAM: an implementation of the weighted histogram analysis method. *University of Rochester, USA* **2011**.
48. Kan, S. B. J.; Lewis, R. D.; Chen, K.; Arnold, F. H., Directed evolution of cytochrome c for carbon–silicon bond formation: Bringing silicon to life. *Science* **2016**, *354* (6315), 1048–1051.
49. Berry, E. A.; Trumpower, B. L., Simultaneous determination of hemes a, b, and c from pyridine hemochrome spectra. *Anal. Biochem.* **1987**, *161* (1), 1–15.
50. Kille, S.; Acevedo-Rocha, C. G.; Parra, L. P.; Zhang, Z.-G.; Opperman, D. J.; Reetz, M. T.; Acevedo, J. P., Reducing Codon Redundancy and Screening Effort of Combinatorial Protein Libraries Created by Saturation Mutagenesis. *ACS Synth. Biol.* **2013**, *2* (2), 83–92.
51. Ito, M.; Itazaki, M.; Abe, T.; Nakazawa, H., Hydrogenation of Chlorosilanes by NaBH₄. *Chem. Lett.* **2016**, *45* (12), 1434–1436.